



Interfacial bond strength and failure modes of traditional and modern repair materials for historic fibrous plaster

Barrie Dams · Naveen Kumar · Rajnish Kurchania · John Stewart ·
Martin Ansell · Marion Harney · Richard J. Ball

Received: 1 February 2023 / Accepted: 29 August 2023 / Published online: 13 September 2023
© The Author(s) 2023

Abstract Many culturally important historic buildings contain fibrous plaster ceilings. The collapse at London's Apollo Theatre in 2013, which injured 88 people, highlighted the importance of inspecting and restoring ceilings effectively. This study focuses on traditional and modern materials which are applied to the topsides of existing historic fibrous plaster ceiling elements during repair and maintenance. Fibrous plaster ceilings are commonly suspended from primary or secondary structural roof members using fibrous plaster wadding ties or 'wads'. The application of additional repair material requires the formation of an interface, defining the strength of the repair. Properties of this interface were evaluated through a novel methodology employing pull-off tests' of approximately 200 specimens consisting of Alpha plaster, Beta plaster, Jesmonite and Aramid gel. Notably, the effect of fibrous reinforcement, and compatibility with historic and degraded material was

also investigated. This study has enabled quantification of interfacial properties and evaluated cohesive and adhesive failure modes. Importantly, the extent of redundancy within historic plaster ceiling practice has been demonstrated, with pull-off occurring from 0.5 kN to 2 kN loading, and the ductile behaviour of repair materials evaluated. Results highlight the importance of surface condition, with clean surfaces exhibiting double the tensile loading capacity compared to soiled (dirty) surfaces representative of those encountered on-site. The significance of this study lies in the quantification of repair material performances and consideration of variations in performance, methodology and in-situ environmental factors. Impact stems from the ability of practitioners to make informed decisions relating to adhesion performance when carrying out repairs. A key outcome is more effective preservation of historic elements in heritage buildings, higher levels of safety and serviceability.

B. Dams (✉) · M. Ansell · M. Harney · R. J. Ball
Department of Architecture and Civil Engineering,
University of Bath, Claverton Down, Bath BA2 7AY, UK
e-mail: bd272@bath.ac.uk

N. Kumar · R. Kurchania
Department of Physics, Maulana Azad National Institute
of Technology, Bhopal, Madhya Pradesh 462003, India

J. Stewart
Historic England, 4th Floor, Cannon Bridge House, 25
Dowgate Hill, London EC1R 2YA, UK

Keywords Fibrous plaster ceilings · Interface ·
Adhesive tests · Pull-off strength · Adhesive failure ·
Cohesive failure

1 Introduction

Fibrous plaster is a composite material which has been used as a decorative element in multiple applications



such as ceilings, panelling and ornamental features since Alexander Desachy patented the invention in 1856 [1], following which it was purchased by George Jackson and Sons within the UK [2]. Fibrous plaster has been used extensively in many period buildings such as theatres, music halls, civic buildings and high-end private residences [3] which are still very much in existence today and heavily used by members of the public. Fibrous plaster ceiling elements are typically suspended by fibrous plaster wadding ties, or simply 'wads', attached to steel or timber structural roof elements [4]. The importance of constantly surveying and maintaining fibrous plaster ceilings was brought into the spotlight when the ceiling of the Apollo theatre, London, UK partially collapsed in 2013, resulting in the injury of 88 people with some serious injuries requiring hospitalisation [5, 6]; this was classed as a major incident by the metropolitan police. The Apollo event was followed by failures in the Savoy theatre, London [7] and numerous other localised failures, many of which are not publicised. An investigation by Westminster Council, London, considered that regular and ongoing surveillance of fibrous plaster ceiling panels and wad elements is required and should be conducted by both fibrous plaster industry specialists and structural engineers [8]. Prior to guidance issued by the Association of British Theatre technicians (ABTT) and regular inspection occurring, fibrous plaster companies were often contacted on an emergency basis to assess ceilings displaying localised failure.

Surveillance and maintenance of fibrous plaster ceilings is performed by a small and specialist plastering industry. Historic roof structures may not be watertight or airtight and moisture and fungal related issues, including plumbing leaks on lower floors, can promote degradation in fibrous plaster elements [9], leading to aged elements requiring repair. Previously to the emergence of fibrous plaster, lime plaster was used as decorative ceilings and elements along with timber laths in historic buildings [10]; in a ceiling application this was typically in a 'lath and plaster' arrangement. The invention of fibrous plaster ultimately replaced lath and lime plaster as the decorative plaster material of choice. Fibrous plaster was quicker to set, allowed for greater spans and thinner panels, and with the use of mouldings a greater range of ornamental arrangements, features and purposes were possible [2].

Fibrous plaster ultimately accelerated production [11] with a change in emphasis from in-situ construction to fabrication in a workshop setting and allowing theatres and civic building decorative elements to be realised more quickly and efficiently, promoting economic viability. During the 1860–1930 era of theatre and playhouse building, there was an absence of control measures regarding fibrous plaster works, with work being designed and self-certified by contemporary fibrous plaster companies.

Fibrous plaster wads and ceiling panels consist of gypsum plaster (traditionally 'beta' gypsum plaster mined from the Montmartre quarry near Paris, France, leading to the well-known term 'Plaster of Paris') [12], hessian fibre scrim consisting of fibres woven in orthogonal directions which come from the Jute plant [13] and a galvanised steel wire in wads. However, it has been noted by modern surveillance that the vast majority of historical fibrous plaster wads in period building ceilings were installed without steel wire included, suggesting that historically it was considered normal or acceptable practice to use just plaster and hessian fibres. Steel wire could be used to secure casts in place, but wire was not galvanised prior to 1920. It is now common and recommended in modern commercial practice to use steel wires [14] when installing new wads to replace aged ones. Fibrous plaster ceiling elements also included reinforcing timber laths around the perimeter of panels, enabling the alignment of adjacent panels, and also at regular spacings within panels in orthogonal directions. There is also a modern plaster variation known as 'Alpha' plaster which is stronger and has been manufactured since the 1930s [15]. Ceiling panel elements are not necessarily flat; elements can also be sloped and include signature features such as domes.

Hessian fibre scrim is a traditional method of providing reinforcement in fibrous plaster and is still used today in wad repair applications and new fibrous plaster panel and decorative elements. The Jute plant is mainly found in India, with Dundee in Scotland, UK, historically being a major centre for the jute industry and production of products such as woven hessian scrim from the mid-1800s [14]. Alternative plant materials such as sisal have also been used in other countries. The use of fibres provides several advantages—fibres provide tensile strength to the cast and introduce ductility as part of a composite material as opposed to the brittle nature of the plaster matrix



alone. Fibres also hold supporting timber laths in position within cast ceiling panels (reinforcing timber laths are typically spaced at 0.5 m in a fibrous plaster ceiling element), fibres also are crucial elements of wadding ties attaching ceiling panels to supporting timber or steel structural members and fibre scrim soaked in plaster form overlapping joints between adjacent panel elements manufactured separately and joined in-situ [3, 15].

Figure 1 contains images of a section through a fibrous plaster element and hessian fibre along with in-situ fibrous plaster ceilings and illustrations of the different repair applications. Figure 1a illustrates a section through a fibrous plaster element showing layers of hessian scrim, with Fig. 1b showing a close-up drawing of a hessian fibre structure [15]. Figure 1c shows the decorated underside of a fibrous plaster ceiling.

There are three core methods of repair in modern practice. The first is the application of new fibrous plaster wads in-situ to support the ceiling panels and effectively replace degraded historical wads. The second method is the application of plaster (or an alternative modern acrylic-modified material) and fibre scrim to reinforce degraded fibrous plaster; soaked, wetted scrim can be placed as laminations to form a thickness of 1.2 mm in desired areas on top of historic material in-situ. Repair material can also be locally applied by brush. Thirdly, repair material can be applied by spraying material onto the topside of fibrous plaster elements in-situ to a thickness of 1.5 mm (taking care while spraying to avoid any visual coverage of structural elements).

Figure 1d-f images show ceiling topside images showing the different repair methods. Figure 1d shows newly applied wads consisting of gypsum plaster, hessian fibres and galvanised steel draped over structural supporting timber beams and affixed to the topside of a historic ceiling, with new plaster in contact with aged plaster. The topside of a historic ceiling may be well over a century old and be covered in accumulated layers of mould and dirt. This may have a significant influence of the mechanical integrity of the interface between any newly applied repair material and the topside of the in-situ ceiling panel element. In modern practice, it is typical to vacuum the topside of historic fibrous plaster ceilings to remove the layers of mould and dirt which have built up over the years and providing it is safe to do so by inspection,

carefully inscribe lines to form a mechanical 'key' to roughen the topside surface to aid adhesion of a newly applied material and promote bonding. Figure 1e illustrates the application of a lamination consisting of a fibrous scrim with quadaxial glass fibres as a replacement for traditional hessian, soaked in an acrylic-modified plaster and placed upon in-situ historic material. Figure 1f features a gel material which has been sprayed onto the topside of a historic ceiling to a thickness of 1.35 mm.

This study concerns the methods of repairing and reinforcing fibrous plaster ceilings and focuses upon the interfacial region and bonding between the repair material and in-situ aged material. To the author's knowledge no previous studies of the interfacial bonding or adhesion tests have been undertaken, therefore this study forms a vital contribution to complement the surveying and repairing of historic fibrous plaster ceilings, providing quantification and a scientific understanding of the adhesive and tensile properties of the repair of fibrous plaster elements along with potential modes of failure. All repair methods and materials utilised in this study are established, effective and representative of ongoing methods of repair in commercial practice. This study complements commercial experience and empirical knowledge with robust analysis under laboratory conditions. The data provides a greater understanding of the interfacial properties of repair materials and furthermore compatibility with historic fibrous plaster material. Four different material repair systems were studied; in addition to using Beta plaster and Alpha plaster as matrix materials, modern alternatives Jesmonite and Historic Plaster Conservation Products (HPCP) RE Aramid GelTM were also investigated. These four materials are salient methods all used by different commercial companies but are not entirely representative of all materials in worldwide use.

Jesmonite has been used as an alternative to traditional gypsum plaster for repair applications. Invented by Peter Hawkin in the early 1980s with the development of the product AC100, Jesmonite is an acrylic-modified gypsum plaster composite material consisting of two components; a reactive mineral base (powder component) and a water-based acrylic resin (liquid component). When the components are mixed, it can be applied in a varied palette of colours, textures, and finishes [16]. The acrylic-modified gypsum composite material has been used in conjunction with

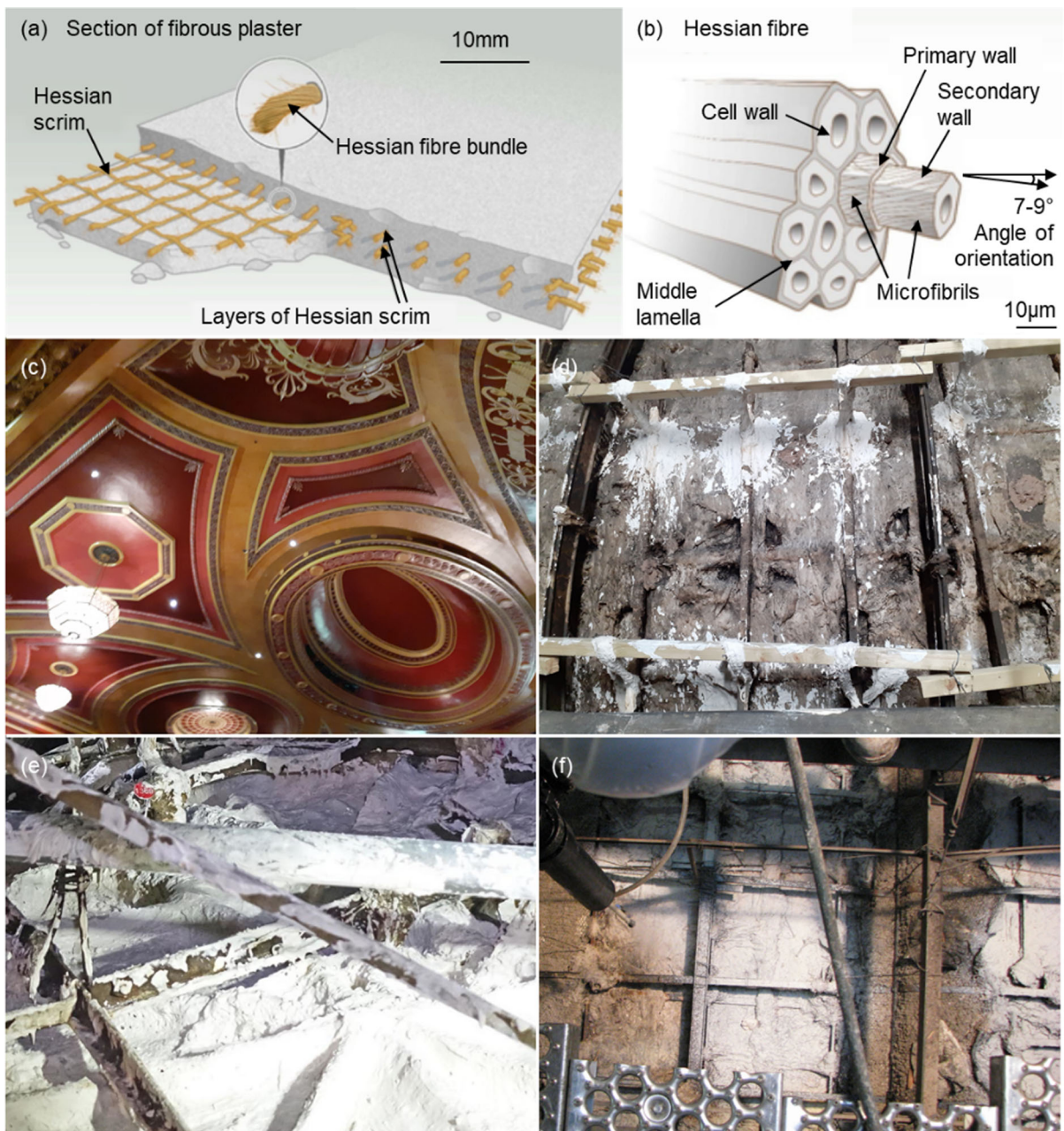


Fig. 1 Historic fibrous plaster ceiling structure and examples of modern repair methods. **a, b** Axonometric drawing of fibrous plaster element with hessian scrim and illustration of hessian fibre structure (Source: [15]). **c** A theatre's fibrous plaster ceiling underside showing decoration and ornate features (Source: Author). **d** An example of newly applied fibrous plaster

composite wads (Source: Author). **e** Laminations of an acrylic modified plaster with alkali-resistant quadaxial fibreglass reinforcement on the topside of a ceiling (Source: [12]). **f** The application by spraying of a thin lamination of HPCP RE Aramid Gel™ on to a ceiling topside (Source: [18])

quadaxial fibre reinforcement to give a moisture resistant modern material option for the repair and conservation of traditional fibrous plaster elements

[12] and applied in thin laminations as shown in Fig. 1e.

HPCP RE Aramid GelTM is a further modern repair alternative for traditional plaster, which has been used in applications in North America as a complete repair system. Patented in both the United States and Canada, it was invented in 2010 by Rod Stewart of the company HPCP, which have been creating plaster conservation products since the 1980s. It is typically applied by spraying a thin 1.5 mm thick layer on to the topside of the traditional ceiling panel surface which requires repair, resulting in a dried thickness of 1.35 mm; this allows coverage over a wide area as depicted in Fig. 1f. Typically, an in-situ panel topside is initially keyed to increase bonding surface area and an acrylic primer HPCP CO S-20TM is applied prior to HPCP RE Aramid GelTM application, which contains DuPontTM Kevlar® fibres as part of the gel product, used in commercial application to promote the bonding of the repair material to the historic material topside. The term ‘RE’ denotes a reinforcing material and the term ‘CO’ denotes that the primer is a consolidating material [17]. The material can also be used to spray on to existing in-situ wads, encapsulating the whole surface and reinforcing the historic wads with tensile properties; this study focuses on the adhesive bonding strength in the new material-existing panel material interfacial region.

Fibreglass quadaxial fibres are a synthetic modern option to replace traditional hessian fibres in fibrous plaster elements. Quadaxial fabrics are comprised of four layers oriented typically at 0°/90° and +45°/−45°. Awang-Ngah et al. 2019, investigated both new hessian fibres and quadaxial fibres in flexural strength tests and the two fibre types performed quite similarly in terms of flexural strength [13], suggesting that quadaxial fibre scrim is an appropriate and sympathetic modern alternative to the traditional hessian scrim. Quadaxial fibres can be placed on the topside of an existing ceiling in-situ requiring repair and used in conjunction with an overlay of new gypsum plaster [15] or acrylic polymer modified plaster, with typically 2–3 layers of modified plaster-soaked fibre mats. Quadaxial fibres have a cost implication and are a more expensive option than natural hessian fibres but offer greater resistance to moisture and fungal attack degradation than natural plant-based fibres.

2 Methodology

A series of adhesion ‘pull-off’ tests specimens were manufactured to be representative of four materials currently used in historic fibrous plaster conservation in the UK and North America—Alpha plaster, Beta plaster, HPCP RE Aramid GelTM and Jesmonite. Pull-off tests are suitable for evaluating the bonding of repair applications of concrete [19] and pull-off test methodology [20] has been adapted by the authors for this study. Each material was applied to both ‘clean’ new plaster and ‘dirty’ simulated soiled plaster surfaces. Soiled plaster surfaces were simulated by applying a layer of dust and dirt sourced from an historic roof void to the plaster bases. Figure 2a and b contain Scanning Electron Microscopy (SEM) images at × 100 and × 500 magnifications detailing the highly uneven and varying topography resulting from decades of accumulated dirt on a historic fibrous plaster ceiling element topside. X-Ray Diffraction (XRD) was carried out to determine the crystalline structure of the roof dirt along with manual sieving to establish a particle size distribution. XRD analysis revealed the dirt to largely consist of quartz (SiO₂) with some CaCO₃ and traces of organic material. Figure 2c depicts the XRD spectrum showing the quartz peaks and Fig. 2d shows the particle distribution tests and range of particle sizes in the roof dirt.

2.1 Test specimens design, materials and matrix of sample groups

Figure 3a illustrates the tensile ‘pull-off’ test specimen design and dimensions, which consisted of a 150 mm × 150 mm × 35 mm beta gypsum plaster base, on to which a cylinder of 50 mm Ø and up to 5 mm thickness of each test material was applied.

The roof void dirt was applied 5 min after initial casting while the plaster was still soft. After a further 10 min loose dirt was removed using a soft brush. The resulting surface was impregnated with a thin layer of dirt. The method and approach of applying the dirt to the bases was unanimously agreed by the authors with the four commercially active independent companies which helped to manufacture the test specimens. The application of the roof dirt was considered to be representative of a vacuum-cleaned in-situ fibrous plaster panel element topside and the methodology of dirt application was kept consistent across all sample

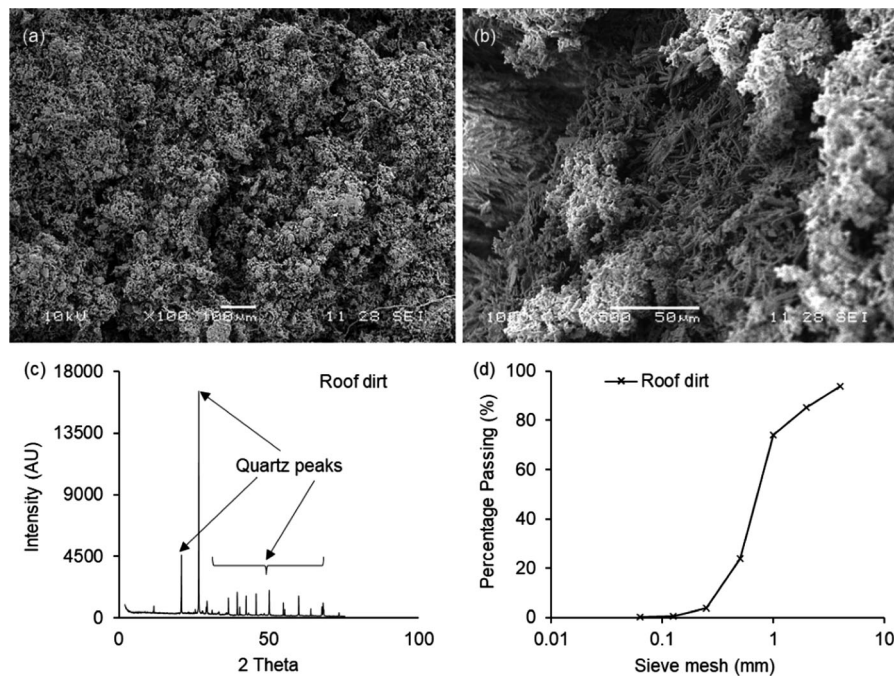


Fig. 2 a, b SEM images at $\times 100$ and $\times 500$ respectively of in-situ dirt on a fibrous plaster element (Source: Authors). c XRD spectrum of the roof dirt, revealing it is predominantly

comprised of quartz. (d) Particle size distribution of the roof dirt showing the range of sizes

groups made by the different companies. In addition, a plaster base was formed from a section of actual ceiling removed from a theatre. Dirty bases represent in-situ historic material on to which new, repair material is applied (represented by the 50 mm \varnothing cylinder); the clean bases enabled comparisons to be made.

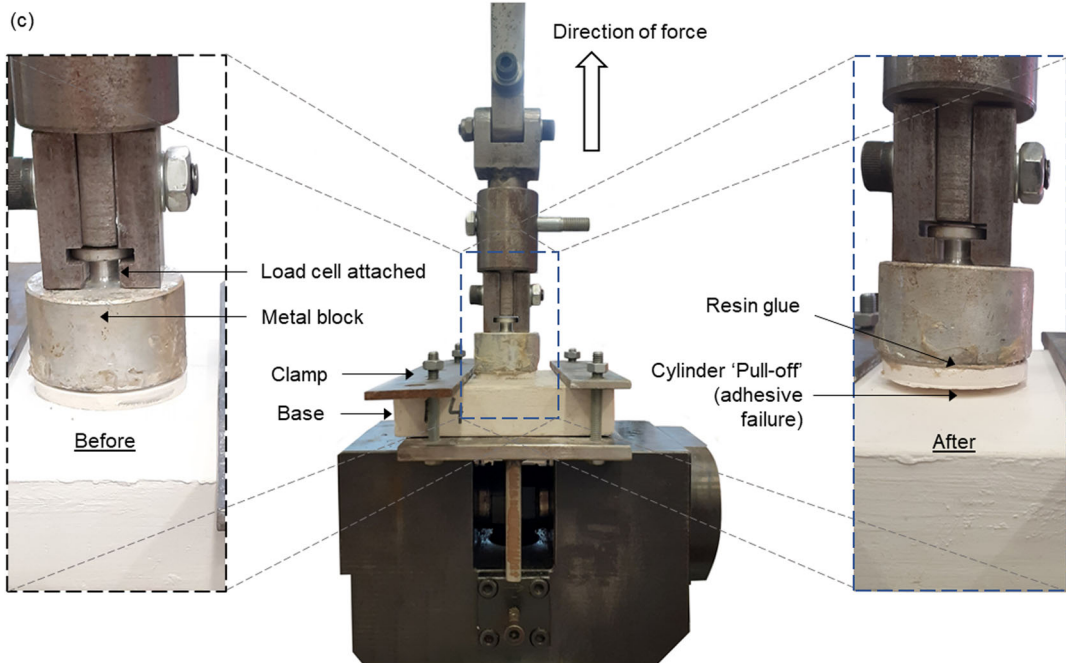
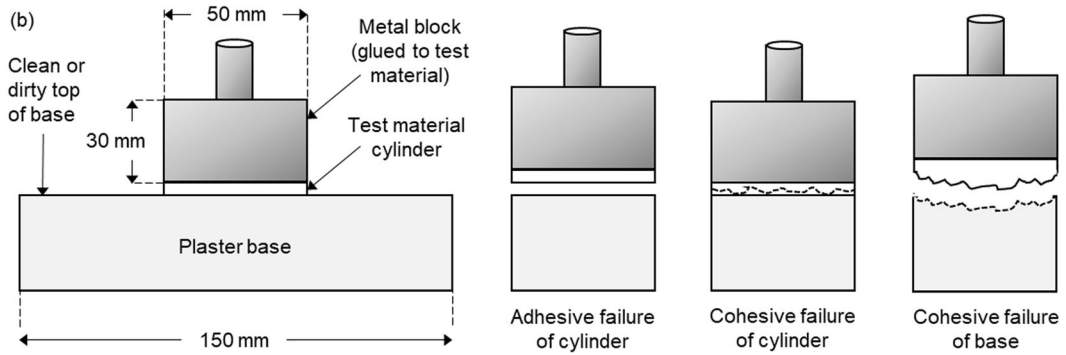
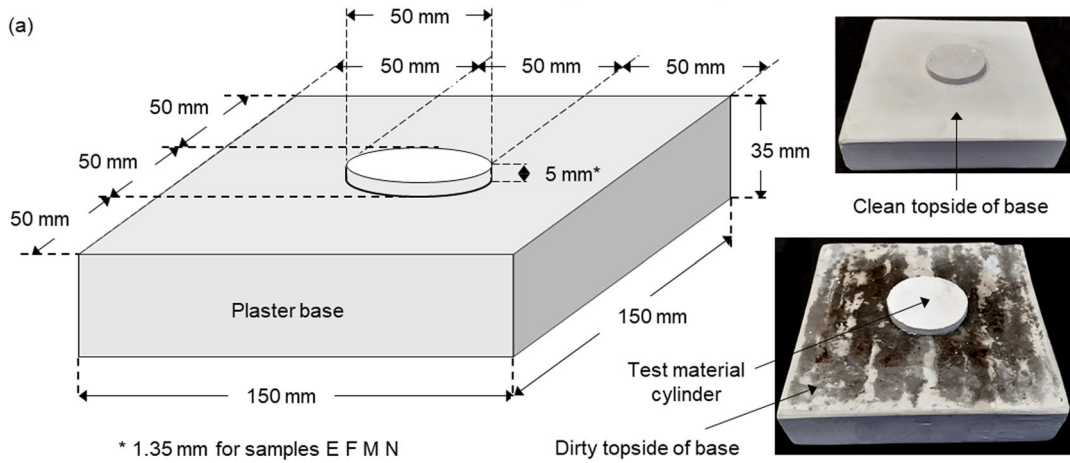
Table 1 shows the full matrix of sample groups for the tensile pull-off tests, with sample groups named by a coding system of matrix material—fibres (if present)—clean or dirty base (CB or DB respectively). Twelve specimens were manufactured for each sample group, with the exception of six specimens for the historic base group as this was from a finite supply of historic material salvaged from a building during conservation work. A total of 198 specimens were tested as part of this study.

Alpha plaster groups begin with 'AP': These sample groups represent Alpha plaster with (and without) reinforcing quadaxial fibres being applied to the topside of historic ceilings as repair material option, or a plaster-soaked scrim applied directly to repair an aged element, with the new Alpha plaster in contact with the aged plaster. There are different alpha

plasters commercially available with properties that will vary, the type used for this study was Crystacal® 'R'. QF denotes the presence of quadaxial fibres. As an example: AP-QF-CB denotes Alpha plaster with quadaxial fibres on a clean base.

Beta plaster groups begin with 'BP': These sample groups represent Beta plaster along with hessian fibres forming fibrous plaster wads and the practice of affixing new wads by operatives in a roof space to the topside of a historic ceiling in-situ, or a plaster-soaked scrim applied directly to repair an aged element with the new Beta plaster in contact with aged, dirty historic plaster. HF denotes the presence of hessian fibres. As an example, BP-HF-DB denotes Beta plaster with hessian fibres on a dirty base.

HPCP RE Aramid Gel™ groups begin with 'AG': These samples represent HPCP RE Aramid Gel™ with DuPont™ Kevlar® fibres (KF) and the associated HPCP CO S-20™ acrylic primer being in contact with aged plaster. This is a conservation product applied to the topside of fibrous plaster elements to a wet thickness of approximately 1.35 mm resulting in a dry thickness of approximately 1 mm. This sample group varies from the matrix—fibres—base



◀ **Fig. 3 a** Isometric view with dimensions of the pull off test sample along with images of both clean and dirty topsides of the plaster base, **b** Modes of failure possible with the metal block secured to the cylinder of testing material with a resin and **(c)** The tensile test rig comprising the adhesion of an aluminium metal block to the sample group specimen and load cell and application of tensile load

Table 1 Matrix of tensile 'pull-off' test samples, showing sample groups defined by code denoting 'cylinder matrix material—Fibres (if present)—Clean or dirty plaster base',

Cylinder matrix material applied to Beta plaster bases	Clean bases (CB) Sample group coding and number of specimens	Dirty bases (DB)	Historic bases (HB)
Alpha plaster (AP)	AP-CB 1-12	AP-DB 1-12	
Alpha plaster (AP) with quadaxial fibres (QF)	AP-QF-CB 1-12	AP-QF-DB 1-12	
Beta plaster (BP)	BP-CB 1-12	BP-DB 1-12	BP-HB 1-3
Beta plaster (BP) with hessian fibres (HF)	BP-HF-CB 1-12	BP-HF-DB 1-12	BP-HF-HB 4-6
HPCP RE Aramid Gel™ (AG) with DuPont™ Kevlar® fibres (KF) + acrylic primer HPCP CO S-20™	AG-KF-CB 1-12	AG-KF-DB 1-12	
Just HPCP CO S-20™ acrylic primer (P) (without the HPCP RE Aramid Gel™) (AG-P)	AG-P-CB 1-12	AG-P-DB 1-12	
Jesmonite (J)	J-CB 1-12	J-DB 1-12	
Jesmonite (J) with quadaxial fibres (QF)	J-QF-CB 1-12	J-QF-DB 1-12	

Sample groups beginning 'AG' vary from the matrix—fibres—base abbreviation formula due to the fibres being intrinsically part of the gel product and the primer additionally tested in isolation from the gel/fibre product. Therefore, for HPCP RE Aramid Gel™ (AG) with intrinsic DuPont™ Kevlar® fibres (KF) and the accompanying HPCP CO S-20™ acrylic primer being used, AG-KF-CB/DB adheres to the matrix—fibres—base formula. However, the sample group using just the primer (with no gel/fibres) varies from the formula and is denoted AG-P-CB/DB, keeping 'AG' to signify it is part of the overall HPCP RE Aramid Gel™ group, and 'P' denoting just the use of the 'Primer', with clean (CB) or dirty base (DB) remaining as per the abbreviation formula

abbreviation formula due to the fibres being intrinsically part of the gel product and not added separately, and the primer being also tested in isolation from the gel/fibre product. Therefore, for HPCP RE Aramid Gel™ with intrinsic DuPont™ Kevlar® fibres (KF) and the associated HPCP CO S-20™ acrylic primer being used, AG-KF-CB/DB adheres to the matrix—fibres—base formula. However, the sample group

using *just* the primer (with no gel/fibres) varies from the formula and is denoted AG-P-CB/DB, keeping the 'AG' to signify it is part of the overall HPCP RE Aramid Gel™ group, and 'P' used to denote *just* the use of the 'Primer', with clean (CB) or dirty base (DB) remaining as per the abbreviation formula.

with each group having 12 test specimens (note: Historic base sample groups BP-HB and BP-HF-HB have 3 specimens each)

Jesmonite groups begin with 'J'; this is another alternative modern synthetic material which can be applied with quadaxial reinforcing glass fibres to the topside of a historic ceiling in-situ; these sample groups represent Jesmonite being used as an acrylic-modified gypsum composite material being in contact with aged plaster. There is a sample group both with and without quadaxial fibres (QF). As an example,



Table 2 Selected material properties of the constituent materials involved in the tests conducted in this study

Material	Density (kg/m ³)	Time to set (mins)	Plaster to water ratio	Compressive strength (MPa)	Tensile strength (MPa)	Flexural strength (MPa)	Youngs modulus	Source(s)
Beta plaster	885	10	100:66–71	13	–	3–5	3–5 (GPa)	[15] [21]
Alpha plaster (Crystacal® R')	1100	15–18	100:35	55	–	6–9	8–10 (GPa)	[22] [23]
Jesmonite	1745	15–20	2.5:1 (Base: Liquid)	25–30	25–35	50–65	5–6 (MPa)	[24] [25]
RE aramid gel—Kevlar fibres	1050 (gel) 1440–1460 (fibres)	–	–	517	2800–2920 (Tensile modulus 70 GPa)	N/A	4 (GPa)	[26] [27] [28]
Quadaxial fibres	2600	–	–	–	1700	2	3.5–4.5 (GPa)	[29] [15]
Hessian fibres	1400	–	–	–	200–700 (Tensile modulus 13–30 GPa)	1	3–4 (GPa)	[15] [30] [31] [32] [28]

J-DB denotes Jesmonite with no fibres added on a dirty base.

Table 2 summarises selected material properties for the materials used in this study including density along with compressive, flexural and tensile strengths; values are drawn from previous studies (including by the authors) and manufacturer's literature and specifications.

2.2 Specimen plaster base manufacture

The bases of the specimens for the sample groups were manufactured according to the following methodology:

2.2.1 Manufacture of clean bases (CB)

1. Beta gypsum plaster, mimicking historical material, was mixed and the base mould filled with fresh material.
2. Once a 'tacky' consistency was attained by the fresh material, the top of the mould was struck to create a level top surface.
3. Process repeated to create a total of 96 clean base specimens.

2.2.2 Manufacture of dirty bases (DB)

1. Samples of historic in-situ roof void dirt/mould were collected and sieved.
2. The sieved samples of roof void dirt were weighed to ensure a total in excess of 288 g, with 3 g applied to each of the 96 'dirty' topsides of the base specimens in sample groups ending DB.
3. Beta gypsum plaster was mixed and the base mould filled with fresh material.
4. Once a 'tacky' consistency was attained by the fresh material, 3 g of dirt was evenly applied on top of the base plaster, ensuring particularly good cover in the central region where the test cylinders of new material were to be applied.
5. After a five minute pause, the top of the base samples were struck to attain a level surface.
6. More dirt was then rubbed into the base plaster with a firm brush, with an even application over the entire sample.
7. Process repeated to create a total of 96 dirty base specimens.

2.2.3 Manufacture of specimen bases for historic plaster base groups (ending (HB))

1. A historic plaster element was cut into as many base pieces as possible to satisfy the base dimensions of 150 mm × 150 mm × 35 mm thickness—with six specimen base plates achieved.
2. The historic elements were cleaned with a Hoovering device as is standard commercial practice and a ‘key’ was applied (scratching to roughen the surface and aid adhesion).
3. Historic base samples were placed into the base mould and fresh plaster was poured in to surround the historic base to provide straight edges for the base to fit smoothly and evenly into the test rig.

2.2.4 Specimen pull-off cylinders manufacture

The pull-off cylinders of the specimens for the sample groups were manufactured according to the following methodology. As fibres, whether hessian or quadaxial glass modern alternatives, would be present in applied repair material matrices, fibres were present within the material applied as cylinders to the test bases (Figure 3); specimens were manufactured both with and without fibres for comparison. Manufacturing methods are presented in the following individual subsections for the four matrix materials Beta Plaster, Alpha Plaster, RE Aramid Gel and Jesmonite.

2.2.5 Manufacture of Pull off cylinder application for Beta plaster groups:

2.2.5.1 Beta plaster only (BP-CB and BP-DB)

1. Primal Rhoplex WS24 primer (1:7 water) was applied to the top surface of the base; this is an acrylic colloidal dispersion in water with small particle sizes (approximately 0.03 μm) for consolidating plaster surfaces, improving the stability of aged friable plasters.
2. Silicone mould with a 50 mm Ø, 5 mm deep circular aperture was fixed on top of the plate.
3. Beta gypsum plaster was mixed and the mould aperture was filled.
4. The top of the mould was struck to provide a flat top to the resulting beta plaster cylinder.
5. Repeated to create 24 specimens.

2.2.5.2 Beta plaster with hessian fibres (BP-HF-CB and BP-HF-DB)

1. Follow steps 1 and 2 as for Beta plaster only.
2. Beta gypsum plaster was mixed and the mould aperture was partially filled with a first coating, termed ‘firstings’.
3. Hessian fibre scrim was placed on top of the firstings.
4. A second coat of plaster (‘seconds’) was added to the top of the mould.
5. The top of the mould was struck to provide a flat top to the resulting beta plaster cylinder.
6. Repeated to create 24 specimens.

2.2.5.3 Applying Beta plaster cylinders to historic plaster bases (BP-HB and BP-HF-HB)

1. Follow steps 1 and 2 for Beta plaster only to the rough surface of the historic base.
2. BP-HB: mould filled and struck as per steps 3 and 4 for Beta plaster only.
3. BP-BF-HB: mould filled and struck as per steps 3, 4 and 5 for Beta plaster with hessian fibres.

2.2.6 Manufacture of pull off cylinder application for alpha plaster groups

2.2.6.1 Alpha plaster only (AP-CB and AP-DB) Similar method for groups BP-CB and BP-DB but substituting Crystacal® ‘R’ Alpha Plaster for Beta Plaster for the cylinder formed in the mould aperture.

2.2.6.2 Alpha plaster with quadaxial fibres (AP-QF-CB and AP-QF-DB) Similar process for groups BP-HF-CB and BP-HF-DB but substituting Crystacal® ‘R’ Alpha Plaster for Beta Plaster and quadaxial fibres instead of hessian fibres to form the cylinder in the mould aperture.

2.2.7 Manufacture of pull off cylinder application for HPCP RE Aramid Gel™ groups

The HPCP RE Aramid Gel™ product is an acrylic resin which contains DuPont™ Kevlar® fibres as an intrinsic part of the product; therefore, it was not possible to test the gel material both with and without fibres. It was decided that the performance of the HPCP CO S-20™ acrylic primer, typically applied to



the topside of an in-situ element first before the HPCP RE Aramid GelTM material is sprayed on, also warranted investigation. Therefore, the four sample groups involving gel and associated primer were classified as follows:

- AG-KF-CB: HPCP RE Aramid GelTM with DuPontTM Kevlar[®] fibres, HPCP CO S-20TM acrylic primer, clean base
- AG-P-CB: HPCP CO S-20TM acrylic primer only, clean base
- AG-KF-DB: HPCP RE Aramid GelTM with DuPontTM Kevlar[®] fibres, HPCP CO S-20TM acrylic primer, dirty base
- AG-P-DB: HPCP CO S-20TM acrylic primer only, dirty base

The samples were made in accordance with the following methodology:

1. The topside of the clean and dirty plaster base topsides were lightly vacuumed.
2. A 1.35 mm thick poly-carbonate mould with a 50 mm Ø aperture in its centre was held on the topside of the plaster base.
3. A scribe was used to lightly mark the perimeter of the central circle and to scratch random indentations into the centre of the circle to aid adhesion of the applied materials.
4. A bench brush was applied to lightly brush the circle post-scribing.
5. HPCP CO S-20TM primer was applied with a small brush to the 50 mm Ø circle on the base topside and allowed to penetrate. Ultimately, a small pool of primer was left to coalesce on the surface and penetrate. This represents normal practice of applying primer to the topside of fibrous plaster as the first step after vacuum cleaning.
6. AG-KF-CB and AG-KF-DB only:
 - a. An hour after primer application, a putty knife was used to apply gel to the exposed primer. The knife, with a cutting edge wider than 50 mm was used to strike off excess product and leave a wet-thickness layer of 1.35 mm of material in the circular aperture of the mould. Spray application, the designated commercial technique, was not feasible with specialist apparatus.
 - b. The product was allowed to dry for 24 h leaving a dry thickness of approximately 1 mm.

2.2.8 Manufacture of Pull off cylinder application for Jesmonite groups

Jesmonite only (J-CB and J-DB).

Similar process to Beta plaster groups but substituting the two mixed components of Jesmonite for Beta plaster and water to form the 50 Ø mm cylinder in the mould aperture.

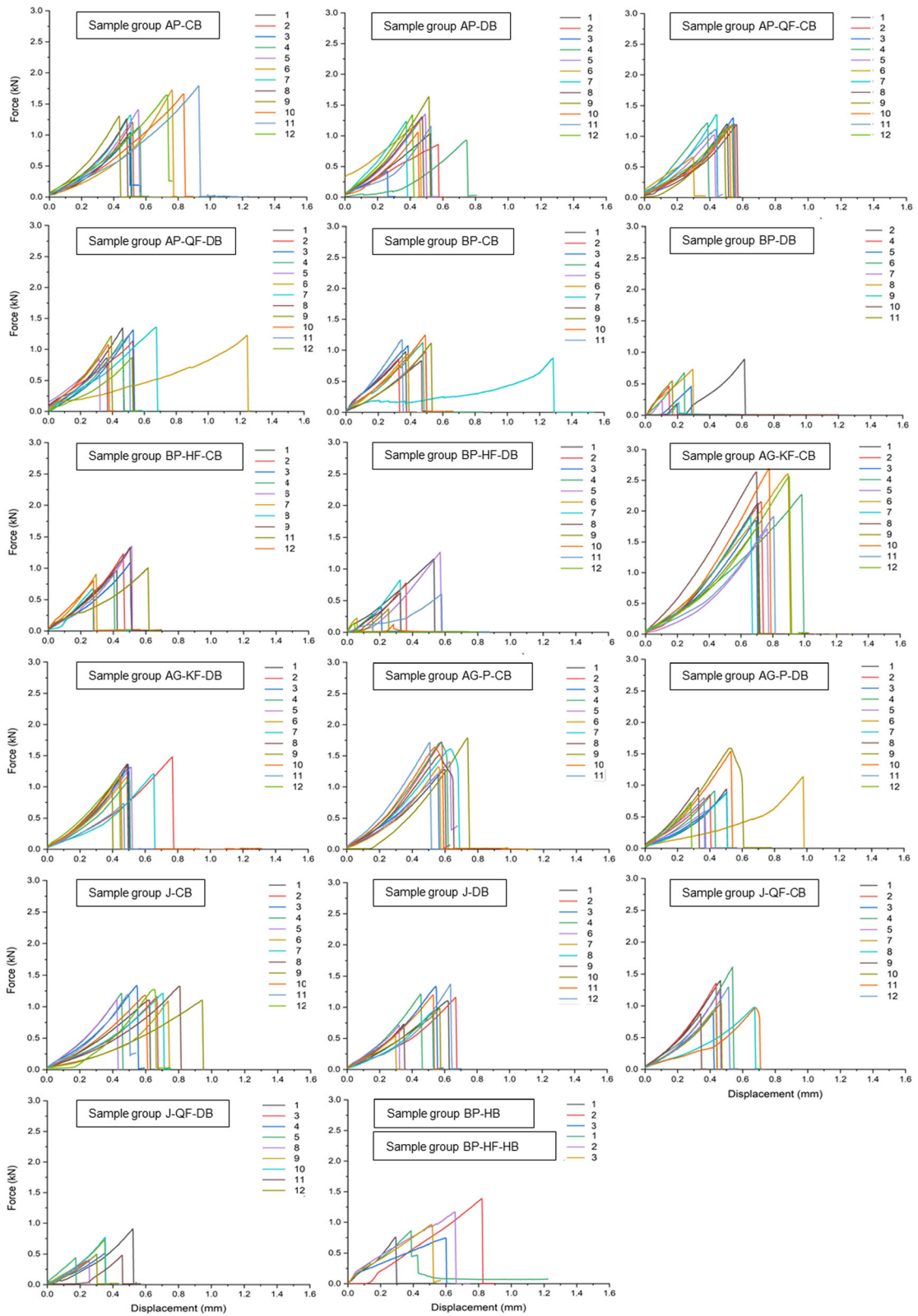
Jesmonite with quadaxial fibres (J-QF-CB and J-QF-DB).

Similar process for Beta plaster groups but substituting Jesmonite components for Beta plaster/water and quadaxial fibres instead of hessian fibres to form the cylinder in the mould aperture.

2.3 Design of the tensile test rig and experimental method

Figure 3b and c illustrate the potential failure modes and the details of the tensile test rig for the pull-off tests. The tensile test rig was based upon BS 1881–207:1992 pull-off test methodology and Fig. 1c [20]. A 50 mm Ø aluminium metal block was mounted centrally on to the cylinders affixed to the base plates using a two component Sikadur -31 epoxy building adhesive (stronger than the cylinder-base bond to ensure that failure did not occur at the metal block—cylinder interface). The aluminium metal block was inserted into a custom-built testing rig. Displacement-controlled tests were carried out using a Dartec Universal Testing machine with a 100 kN load cell and executed at a crosshead speed of 0.2 mm/min until failure occurred. A small pre-load (0.03 kN ± 0.01 kN) was applied after samples were manoeuvred into position to test correct alignment prior to full loading. Failure type (FT), as illustrated in Fig. 3b, was to be classed as either adhesive failure at the cylinder-base interface, cohesive failure within the applied cylinder (resulting in a partial or total fracture within the cylinder material itself and cylinder material being left on the base) or cohesive failure within the base plate (resulting in material being pulled out of the base plate and being attached to the cylinder material).

It could also be possible tests might exhibit partial cohesive failure where part of the cylinder surface area of the base material could be observed having left the base plate and being present on the underside of the pulled off cylinder, the remaining surface area therefore showing adhesive failure. Equally, part of the



◀ **Fig. 4** Matrix of force versus displacement curves for all tested specimens of each sample group

surface area of the applied cylinder material could be observed as being on the base plate, and therefore pulled off from the cylinder. Partial cohesive failures is accompanied by a percentage score, determined by observation, of the surface area of either base material having being pulled off from the base and present on the cylinder, or a percentage of cylinder material having being pulled off from the cylinder and observed on the base. Failure types are coded C for Cohesive failure and A for Adhesive, with CB denoting Cohesive failure in the base material, CC denoting Cohesive failure in the applied cylinder material and partial cohesive failure as A/CB or A/CC followed by the percentage of surface area of material has been removed from the base or applied cylinder.

The maximum force and displacement values for each specimen were recorded. Using the force values, the pull-off stress σ can be calculated as

$$\sigma = \frac{F}{A}$$

where F is the maximum force during loading and A is the cross-sectional area of the 50 mm \varnothing cylinder, taken as 1963.5 mm². OriginLab data analysis software was used to calculate work done (in Joules) using the area below the force—displacement profile of each specimen.

3 Results

Figure 4 illustrates the force—displacement profiles for every specimen tested within the sample groups. Due to displacements being small, occasional visual outliers in terms of the displacement achieved look to be achieving a far greater displacement when the difference remains a fraction of a millimetre. Table 3 shows the maximum force recorded during loading in numerical format for each individual specimen in each sample group along with the mean, standard deviation, coefficient of variation, minimum, median and maximum figure recorded for each sample set.

Figure 5 shows the mean values of the maximum loading results for all tested specimens of the sample groups, with the standard deviation within the sample

represented by the error bars and the coefficient of variation within the sample groups expressed as a percentage and denoted by diamond markers. Using the methodology outlined in Sect. 2.4, the maximum load values are converted to a strength value for the bonding of the cylinders to the bases. Figure 6 shows the mean values of the maximum strength value for the bonding of all specimens within the sample groups, with again standard deviation and the coefficient of variation within the sample groups represented on the figure by error bars and diamond markers respectively. The HPCP RE Aramid GelTM material on clean bases group AG-KF-CB resulted in the highest values of strength and load recorded before specimen failure, with the product applied to dirty bases (AG-KF-DB) recording the second highest mean strength and load totals.

Figure 7 integrates the area under the force—displacement curves shown in Fig. 4 to measure the work done in loading the specimens to failure, expressed in terms of energy (in Joules) for the sample groups, with the standard deviation and coefficient of variation also represented as per Fig. 5 and Fig. 6.

Table 4 shows the entire matrix of test specimens with the failure type (FT) for each specimen determined by observation. Specimens failed in either an adhesive manner A (failure at the cylinder-base interface), cohesive manner C (failure within the base CB, or cylinder CC), or partially cohesive (A/CB or A/CC). Typically in this study, an entirely cohesive failure meant material being pulled out of the plaster base, mainly on clean-base samples, but several examples of cohesive failure in the applied cylinders could be observed in sample group BP-HF-CB.

Numerous specimens exhibited elements of both adhesive and cohesive failure (partial cohesive failure), with the percentage values in the table denoting the approximate surface area of the 50 mm \varnothing cylinder involved, for example a partial cohesive failure CB value of 50% denotes that 50% of the area of the pulled off cylinder had a covering of material pulled off from the base. Typically, full cohesive failure meant a bulk quantity of material was pulled out of the plaster base with thicknesses extending to over 10 mm, whereas typically a partial cohesive failure involved a top/thin layer of material being pulled off to a thickness < 1 mm. Results are further described in individual subsections for each matrix material—Beta

Table 3 Maximum force registered during loading for each individual specimen in the sample groups. The table also shows the Mean, Standard Deviation (ST. D.) Coefficient of Variation (CoV), minimum, Median and Maximum value recorded for each sample set

AP-CB	FORCE (kN)	AP-DB	FORCE (kN)	AP-QF-CB	FORCE (kN)	AP-QF-DB	FORCE (kN)	BP-CB	FORCE (kN)	BP-DB	FORCE (kN)
AP-CB 1	1.035	AP-DB 1	1.031	AP-QF-CB 1	1.203	AP-QF-DB 1	1.339	BP-CB 1	1.031	BP-DB 1	x
AP-CB 2	1.205	AP-DB 2	0.858	AP-QF-CB 2	1.198	AP-QF-DB 2	1.133	BP-CB 2	0.858	BP-DB 2	0.886
AP-CB 3	0.951	AP-DB 3	0.422	AP-QF-CB 3	1.295	AP-QF-DB 3	1.311	BP-CB 3	0.422	BP-DB 3	x
AP-CB 4	1.138	AP-DB 4	0.928	AP-QF-CB 4	1.211	AP-QF-DB 4	1.173	BP-CB 4	0.928	BP-DB 4	0.461
AP-CB 5	1.406	AP-DB 5	1.347	AP-QF-CB 5	1.01	AP-QF-DB 5	0.848	BP-CB 5	1.347	BP-DB 5	0.459
AP-CB 6	1.728	AP-DB 6	1.216	AP-QF-CB 6	0.658	AP-QF-DB 6	1.221	BP-CB 6	1.216	BP-DB 6	0.676
AP-CB 7	1.321	AP-DB 7	1.234	AP-QF-CB 7	1.351	AP-QF-DB 7	1.358	BP-CB 7	1.234	BP-DB 7	0.23
AP-CB 8	1.262	AP-DB 8	1.306	AP-QF-CB 8	1.185	AP-QF-DB 8	0.86	BP-CB 8	1.306	BP-DB 8	0.727
AP-CB 9	1.304	AP-DB 9	1.633	AP-QF-CB 9	1.106	AP-QF-DB 9	1.212	BP-CB 9	1.633	BP-DB 9	0.203
AP-CB 10	1.662	AP-DB 10	1.059	AP-QF-CB 10	1.165	AP-QF-DB 10	1.075	BP-CB 10	1.059	BP-DB 10	0.181
AP-CB 11	1.796	AP-DB 11	1.148	AP-QF-CB 11	1.115	AP-QF-DB 11	1.239	BP-CB 11	1.148	BP-DB 11	0.545
AP-CB 12	1.648	AP-DB 12	1.335	AP-QF-CB 12	1.192	AP-QF-DB 12	0.864	BP-CB 12	x	BP-DB 12	x
MEAN	1.371	MEAN	1.126	MEAN	1.141	MEAN	1.136	MEAN	1.107	MEAN	0.485
ST. D	0.280	ST. D	0.305	ST. D	0.175	ST. D	0.187	ST. D	0.312	ST. D	0.249
CoV (%)	20.4	CoV (%)	27.1	CoV (%)	15.3	CoV (%)	16.4	CoV (%)	28.2	CoV (%)	51.4
MINIMUM	0.951	MINIMUM	0.422	MINIMUM	0.658	MINIMUM	0.848	MINIMUM	0.422	MINIMUM	0.181
MEDIAN	1.313	MEDIAN	1.182	MEDIAN	1.189	MEDIAN	1.193	MEDIAN	1.148	MEDIAN	0.461
MAXIMUM	1.796	MAXIMUM	1.633	MAXIMUM	1.351	MAXIMUM	1.358	MAXIMUM	1.633	MAXIMUM	0.886
BP-HF-CB	FORCE (kN)	BP-HF-DB	FORCE (kN)	AG-KF-CB	FORCE (kN)	AG-KF-DB	FORCE (kN)	AG-P-CB	FORCE (kN)	AG-P-DB	FORCE (kN)
BP-HF-CB 1	0.971	BP-HF-DB 1	1.158	AG-KF-CB 1	2.123	AG-KF-DB 1	1.356	AG-P-CB 1	1.9	AG-P-DB 1	1.207
BP-HF-CB 2	1.227	BP-HF-DB 2	0.781	AG-KF-CB 2	2.146	AG-KF-DB 2	1.475	AG-P-CB 2	2.629	AG-P-DB 2	1.36
BP-HF-CB 3	1.087	BP-HF-DB 3	0.396	AG-KF-CB 3	1.848	AG-KF-DB 3	1.314	AG-P-CB 3	1.727	AG-P-DB 3	0.925
BP-HF-CB 4	0.889	BP-HF-DB 4	0.283	AG-KF-CB 4	2.268	AG-KF-DB 4	1.111	AG-P-CB 4	2.684	AG-P-DB 4	1.164
BP-HF-CB 5	x	BP-HF-DB 5	1.266	AG-KF-CB 5	1.711	AG-KF-DB 5	1.318	AG-P-CB 5	1.907	AG-P-DB 5	0.73
BP-HF-CB 6	1.251	BP-HF-DB 6	0.225	AG-KF-CB 6	2.602	AG-KF-DB 6	1.153	AG-P-CB 6	2.556	AG-P-DB 6	1.174
BP-HF-CB 7	0.904	BP-HF-DB 7	0.826	AG-KF-CB 7	1.279	AG-KF-DB 7	0.937	AG-P-CB 7	1.317	AG-P-DB 7	0.865
BP-HF-CB 8	0.677	BP-HF-DB 8	0.618	AG-KF-CB 8	1.721	AG-KF-DB 8	0.84	AG-P-CB 8	1.606	AG-P-DB 8	0.961



Table 3 continued

BP-HF-CB	FORCE (kN)	BP-HF-DB	FORCE (kN)	AG-KF-CB	FORCE (kN)	AG-KF-DB	FORCE (kN)	AG-P-CB	FORCE (kN)	AG-P-DB	FORCE (kN)
BP-HF-CB 9	1.329	BP-HF-DB 9	0.369	AG-KF-CB 9	1.194	AG-KF-DB 9	0.88	AG-P-CB 9	1.51	AG-P-DB 9	1.591
BP-HF-CB 10	x	BP-HF-DB 10	0.125	AG-KF-CB 10	1.71	AG-KF-DB 10	0.903	AG-P-CB 10	1.786	AG-P-DB 10	1.54
BP-HF-CB 11	1.006	BP-HF-DB 11	0.604	AG-KF-CB 11	1.323	AG-KF-DB 11	0.591	AG-P-CB 11	1.635	AG-P-DB 11	0.8
BP-HF-CB 12	0.799	BP-HF-DB 12	0.151	AG-KF-CB 12	1.407	AG-KF-DB 12	1.133	AG-P-CB 12	x	AG-P-DB 12	0.724
MEAN	1.014	MEAN	0.567	MEAN	1.778	MEAN	1.084	MEAN	1.932	MEAN	1.087
ST. D	0.210	ST. D	0.380	ST. D	0.440	ST. D	0.260	ST. D	0.475	ST. D	0.301
CoV (%)	20.7	CoV (%)	67.1	CoV (%)	24.7	CoV (%)	23.9	CoV (%)	24.6	CoV (%)	27.7
MINIMUM	0.677	MINIMUM	0.125	MINIMUM	1.194	MINIMUM	0.591	MINIMUM	1.317	MINIMUM	0.724
MEDIAN	0.989	MEDIAN	0.500	MEDIAN	1.716	MEDIAN	1.122	MEDIAN	1.786	MEDIAN	1.063
MAXIMUM	1.329	MAXIMUM	1.266	MAXIMUM	2.602	MAXIMUM	1.475	MAXIMUM	2.684	MAXIMUM	1.591
J-CB	FORCE (kN)	J-DB	FORCE (kN)	J-QF-CB	FORCE (kN)	J-QF-DB	FORCE (kN)	BP-HB	FORCE (kN)	BP-HF-HB	FORCE (kN)
J-CB 1	1.105	J-DB 1	1.105	J-QF-CB 1	1.397	J-QF-DB 1	0.908	BP-HB 1	0.754	BP-HF-HB 1	0.861
J-CB 2	1.149	J-DB 2	1.149	J-QF-CB 2	1.355	J-QF-DB 2	x	BP-HB 2	1.386	BP-HF-HB 2	1.167
J-CB 3	1.334	J-DB 3	1.331	J-QF-CB 3	0.869	J-QF-DB 3	0.576	BP-HB 3	0.742	BP-HF-HB 3	0.962
J-CB 4	1.208	J-DB 4	1.209	J-QF-CB 4	1.604	J-QF-DB 4	0.51				
J-CB 5	1.122	J-DB 5	x	J-QF-CB 5	1.22	J-QF-DB 5	0.436				
J-CB 6	1.084	J-DB 6	0.709	J-QF-CB 6	x	J-QF-DB 6	x				
J-CB 7	1.208	J-DB 7	0.542	J-QF-CB 7	0.964	J-QF-DB 7	x				
J-CB 8	1.318	J-DB 8	0.925	J-QF-CB 8	0.977	J-QF-DB 8	0.407				
J-CB 9	1.098	J-DB 9	0.724	J-QF-CB 9	0.874	J-QF-DB 9	0.73				
J-CB 10	1.182	J-DB 10	0.982	J-QF-CB 10	1.047	J-QF-DB 10	0.764				
J-CB 11	1.197	J-DB 11	1.195	J-QF-CB 11	0.969	J-QF-DB 11	0.48				
J-CB 12	1.274	J-DB 12	1.366	J-QF-CB 12	1.286	J-QF-DB 12	0.496				
MEAN	1.190	MEAN	1.022	MEAN	1.142	MEAN	0.590	MEAN	0.961	MEAN	0.997
ST. D	0.084	ST. D	0.270	ST. D	0.244	ST. D	0.172	ST. D	0.368	ST. D	0.156
CoV (%)	7.1	CoV (%)	26.4	CoV (%)	21.4	CoV (%)	29.1	CoV (%)	38.3	CoV (%)	15.6
MINIMUM	1.084	MINIMUM	0.542	MINIMUM	0.869	MINIMUM	0.407	MINIMUM	0.742	MINIMUM	0.861
MEDIAN	1.190	MEDIAN	1.105	MEDIAN	1.047	MEDIAN	0.510	MEDIAN	0.754	MEDIAN	0.962



Table 3 continued

J-CB	FORCE (kN)	J-DB	FORCE (kN)	J-QF-CB	FORCE (kN)	J-QF-DB	FORCE (kN)	BP-HB	FORCE (kN)	BP-HF-HB	FORCE (kN)
MAXIMUM	1.334	MAXIMUM	1.366	MAXIMUM	1.604	MAXIMUM	0.908	MAXIMUM	1.386	MAXIMUM	1.167

Plaster, Alpha Plaster, Re Aramid GelTM and Jesmonite.

3.1 Beta plaster groups with and without hessian fibres

Figure 8 depicts selected images illustrating the range of failure types from sample groups BP-CB, BP-HF-CB, BP-DB, BP-HF-DB and BP-HB, BP-HF-HB featuring Beta plaster and hessian fibres (note: metal block images with cylinders attached were not available for these sample groups). Figure 8a shows specimens from sample group BP-CB which consisted of beta plaster cylinders on clean bases. Failure types ranged from cohesive failure in the base, where the metal block pulled off a small chunk out of the base (shown in the top image) to adhesive failure in the cylinder-base interface (example in the bottom image) which was the most typical occurrence in group BP-CB. Figure 8b shows specimens from sample group BP-HF-CB, consisting of beta plaster cylinders with hessian fibres on clean bases. This was the one sample group which showed evidence of cohesive failure in the applied cylinder rather than the base, with the top image showing plaster and hessian fibre from the cylinder on the top of the plaster base circular area. Specimens also featured adhesive failure at the cylinder-base interface as shown in the bottom image, with only one specimen in this sample group showing partial cohesive failure with a small quantity of base material being pulled off.

Figure 8c illustrates specimens from sample group BP-DB, Beta plaster on dirty bases. All specimens featured adhesive failure at the cylinder-base interface as shown in the top image, with only two exceptions which showed a small degree of cohesive failure in the base material, with an example shown in the bottom image of base material being pulled off. Figure 8d shows specimens from sample group BP-HF-DB, consisting of beta plaster with hessian fibres on dirty bases; specimens in this sample group all exhibited adhesive failure at the cylinder-base interface (an example of which is shown in the top image), with coverage of dirt remaining in the circle on the base. There were two examples of partial cohesive failure in the base with a small quantity of base material pulled off (bottom image). Figure 8e illustrates specimens from sample group BP-HB, BP-HF-HB both without hessian fibres (above image) and with fibres (below



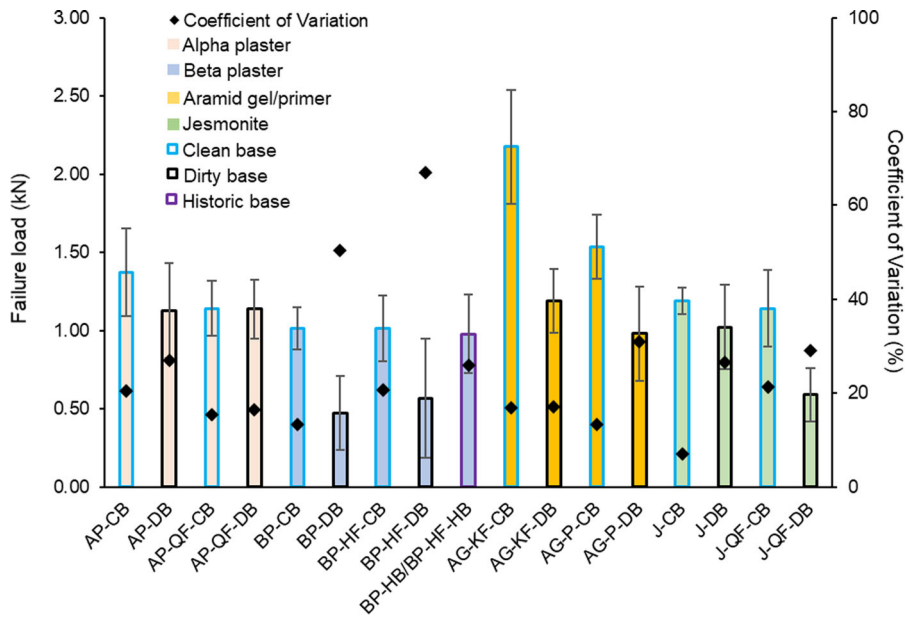


Fig. 5 Mean maximum failure load (force required) of specimens in each sample group, with error bars denoting standard deviation and “black diamond” representing the coefficient of variation

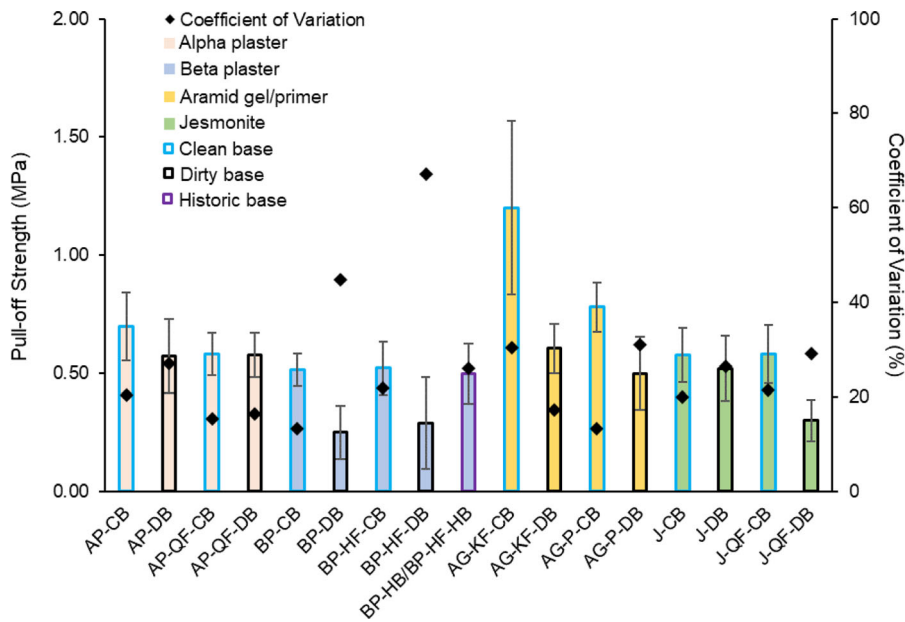


Fig. 6 Mean pull-off strength values of specimens in each sample group, with error bars denoting standard deviation and “black diamond” representing the coefficient of variation

image) with adhesive failure shown in the top image and partial cohesive failure in the bottom image, with an area of the historic base material having been pulled off exposing the historic hessian fibres within.

3.2 Alpha plaster groups with and without quadaxial fibres

Images of selected specimens from sample groups AP-CB, AP-QF-CB, AP-DB and AP-QF-DB showing the

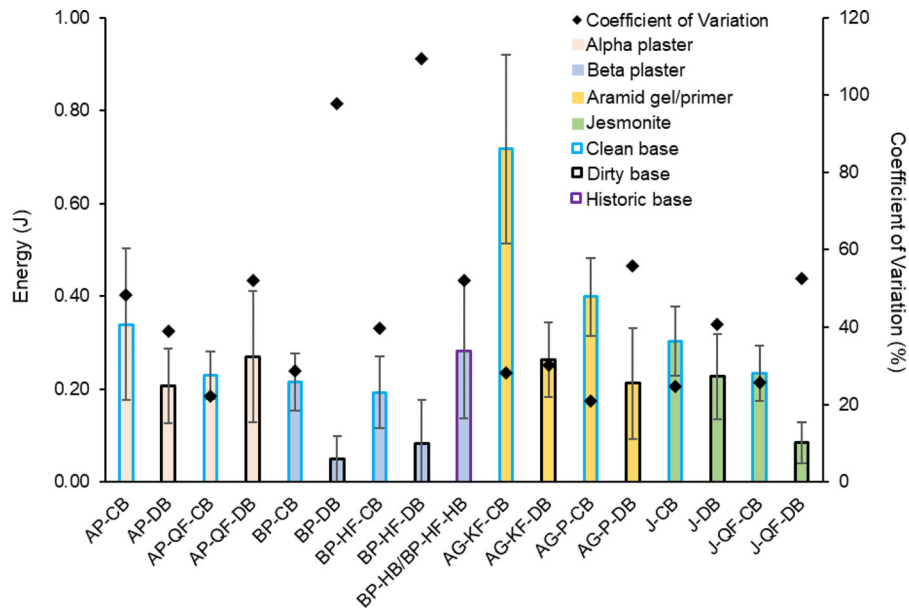


Fig. 7 Mean values of the work done, expressed in energy, of specimens in each sample group, with error bars denoting standard deviation and “black diamond” representing the coefficient of variation

range of failure types are presented in Figure 9. Figure 9a depicts specimens from sample group AP-CB, which featured Alpha plaster on clean bases and showed cohesive failure of the base with varying extents of material pulled out of the base with the least amount pulled out in the top image and the most in the bottom image. Figure 9b shows specimens from sample group AP-QF-CB, which used Alpha plaster with quadaxial fibres on clean bases; again these all showed cohesive failure with varying extents of material pulled out of bases, the least in the top image and most in the bottom image; the set primer applied to the bases prior to the cylinders being affixed can also be seen on the material around the circular area on the metal block in both the top and bottom specimen images.

Figure 9c illustrates specimens from sample group AP-DB, which used Alpha plaster on dirty bases. Group AP-DB largely showed partial cohesive failure in the base, with small quantities of base material being removed, the least amount in the top image, the most in the middle image and in the bottom image is the one instance of cohesive failure in the sample group with a bulk quantity of material pulled from the base; this may be due to less dirt being present in the circular area on this specimen. Figure 9d depicts specimens from sample group AP-QF-DB, with Alpha

plaster and quadaxial fibres on dirty bases. Specimens showed partial cohesive failure with small quantities of base material being removed as shown in the top and middle image; again there was one exception as shown in the bottom image which can be classed as cohesive failure and a bulk quantity of base material pulled off. Figure 9e shows specimens from groups AP-CB (clean base) and AP-DB (dirty base) with the applied cylinders prior to testing.

3.3 HPCP RE Aramid GelTM with DuPontTM Kevlar® fibres and HPCP CO S-20TM acrylic primer groups

Selected images showing the range of failure types from sample groups AG-KF-CB, AG-KF-DB, AG-P-CB and AG-P-DB are shown in Figure 10. Figure 10a illustrates specimens from sample group AG-KF-CB with HPCP RE Aramid GelTM (including DuPontTM Kevlar® fibres) and HPCP CO S-20TM primer on a clean base; this group exhibited both elements of adhesive and cohesive failure to varying extents as shown in both specimen images. Figure 10b shows specimens from sample group AG-P-CB, which featured just primer on a clean base; this sample group ranged from fully cohesive failure (shown in the top image) to partial cohesive failure (lower image).

Table 4 Failure type (FT) for all specimens in each sample group defined in Table 1

AP-CB	FT	AP-DB	FT	AP-QF-CB	FT	AP-QF-DB	FT	BP-CB	FT	BP-DB	FT
AP-CB 1	C	AP-DB 1	A/CB 20%	AP-QF-CB 1	C	AP-QF-DB 1	A/CB 80%	BP-CB 1	A/CB 50%	BP-DB 1	X
AP-CB 2	C	AP-DB 2	A/CB 30%	AP-QF-CB 2	C	AP-QF-DB 2	A/CB 50%	BP-CB 2	A	BP-DB 2	A
AP-CB 3	C	AP-DB 3	A/CB 20%	AP-QF-CB 3	C	AP-QF-DB 3	C	BP-CB 3	A	BP-DB 3	X
AP-CB 4	C	AP-DB 4	A/CB 60%	AP-QF-CB 4	C	AP-QF-DB 4	A/CB 80%	BP-CB 4	A	BP-DB 4	A
AP-CB 5	C	AP-DB 5	A/CB 80%	AP-QF-CB 5	C	AP-QF-DB 5	A/CB 40%	BP-CB 5	A	BP-DB 5	A
AP-CB 6	C	AP-DB 6	A/CB 60%	AP-QF-CB 6	C	AP-QF-DB 6	A/CB 70%	BP-CB 6	A	BP-DB 6	A/CB 20%
AP-CB 7	C	AP-DB 7	A/CB 60%	AP-QF-CB 7	C	AP-QF-DB 7	A/CB 80%	BP-CB 7	X	BP-DB 7	A
AP-CB 8	C	AP-DB 8	A/CB 70%	AP-QF-CB 8	C	AP-QF-DB 8	A/CB 60%	BP-CB 8	A	BP-DB 8	A
AP-CB 9	C	AP-DB 9	A/CB 70%	AP-QF-CB 9	C	AP-QF-DB 9	A/CB 70%	BP-CB 9	A	BP-DB 9	A
AP-CB 10	C	AP-DB 10	A/CB 50%	AP-QF-CB 10	C	AP-QF-DB 10	A/CB 50%	BP-CB 10	A	BP-DB 10	A
AP-CB 11	C	AP-DB 1	A/CB 50%	AP-QF-CB 11	C	AP-QF-DB 11	A/CB 60%	BP-CB 11	C	BP-DB 11	A/CB 30%
AP-CB 12	C	AP-DB 12	C	AP-QF-CB 12	C	AP-QF-DB 12	A/CB 40%	BP-CB 12	X	BP-DB 12	X
BP-HF-CB	FT	BP-HF-DB	FT	BP-HB	FT	AG-KF-CB	FT	AG-KF-DB	FT	AG-P-CB	FT
BP-HF-CB 1	A	BP-HF-DB 1	A/CB 80%	BP-HB 1	A	AG-KF-CB 1	A/CB 50%	AG-KF-DB 1	A/CB 50%	AG-P-CB 1	C
BP-HF-CB 2	A/CC 40%	BP-HF-DB 2	A/CB 40%	BP-HB 2	A 80%	AG-KF-CB 2	A/CB 40%	AG-KF-DB 2	A/CB 40%	AG-P-CB 2	C
BP-HF-CB 3	A	BP-HF-DB 3	A	BP-HB 3	A 60%	AG-KF-CB 3	A/CB 60%	AG-KF-DB 3	A/CB 40%	AG-P-CB 3	C
BP-HF-CB 4	A	BP-HF-DB 4	A	BP-HF-HB	FT	AG-KF-CB 4	A/CB 70%	AG-KF-DB 4	A/CB 50%	AG-P-CB 4	A/CB 30%
BP-HF-CB 5	X	BP-HF-DB 5	A/CB 40%	BP-HF-HB 1	A/CB 50%	AG-KF-CB 5	A/CB 80%	AG-KF-DB 5	A/CB 40%	AG-P-CB 5	A/CB 30%
BP-HF-CB 6	A/CB 30%	BP-HF-DB 6	A	BP-HF-HB 2	A 60%	AG-KF-CB 6	A/CB 50%	AG-KF-DB 6	A/CB 50%	AG-P-CB 6	C
BP-HF-CB 7	A/CC 10%	BP-HF-DB 7	A	BP-HF-HB 3	A/CB 50%	AG-KF-CB 7	A/CB 70%	AG-KF-DB 7	A/CB 70%	AG-P-CB 7	C
BP-HF-CB 8	A	BP-HF-DB 8	A			AG-KF-CB 8	A/CB 50%	AG-KF-DB 8	A/CB 60%	AG-P-CB 8	A/CB 30%
BP-HF-CB 9	A/CC 30%	BP-HF-DB 9	A			AG-KF-CB 9	A/CB 50%	AG-KF-DB 9	A/CB 80%	AG-P-CB 9	A
BP-HF-CB 10	X	BP-HF-DB 10	A			AG-KF-CB 10	A/CB 50%	AG-KF-DB 10	A/CB 50%	AG-P-CB 10	C
BP-HF-CB 11	A/CC 30%	BP-HF-DB 11	A			AG-KF-CB 11	A/CB 80%	AG-KF-DB 11	A/CB 70%	AG-P-CB 11	A/CB 25%
			A								X



Table 4 continued

BP-HF- CB	FT	BP-HF- DB	FT	BP-HB	FT	AG-KF- CB	FT	AG-KF- DB	FT	AG-P- CB	FT
BP-HF- CB 12	A/CC 5%	BP-HF- DB 12				AG-KF- CB 12	A/CB 50%	AG-KF- DB 12	A/CB 70%	AG-P- CB 12	
AG-P-DB	FT	J-CB	FT	J-DB	FT	J-QF-CB	FT	J-QF-DB	FT		
AG-P-DB 1	A/CB 80%	J-CB 1	C	J-DB 1	A/CB 60%	J-QF-CB 1	C	J-QF-DB 1	A/CB 20%		
AG-P-DB 2	A/CB 60%	J-CB 2	C	J-DB 2	A	J-QF-CB 2	C	J-QF-DB 2	X		
AG-P-DB 3	A/CB 70%	J-CB 3	C	J-DB 3	A/CB 80%	J-QF-CB 3	C	J-QF-DB 3	A		
AG-P-DB 4	A/CB 70%	J-CB 4	C	J-DB 4	A/CB 90%	J-QF-CB 4	C	J-QF-DB 4	A/CB 30%		
AG-P-DB 5	A/CB 80%	J-CB 5	A/CB 20%	J-DB 5	X	J-QF-CB 5	C	J-QF-DB 5	A		
AG-P-DB 6	A/CB 80%	J-CB 6	C	J-DB 6	A/CB 95%	J-QF-CB 6	X	J-QF-DB 6	X		
AG-P-DB 7	A/CB 40%	J-CB 7	C	J-DB 7	A/CB 80%	J-QF-CB 7	C	J-QF-DB 7	X		
AG-P-DB 8	A/CB 50%	J-CB 8	C	J-DB 8	C	J-QF-CB 8	C	J-QF-DB 8	A		
AG-P-DB 9	A/CB 10%	J-CB 9	C	J-DB 9	A/CB 90%	J-QF-CB 9	A/CB 40%	J-QF-DB 9	A/CB 60%		
AG-P-DB 10	A/CB 90%	J-CB 10	C	J-DB 10	A/CB 70%	J-QF-CB 10	C	J-QF-DB 10	A/CB 80%		
AG-P-DB 11	A/CB 20%	J-CB 11	C	J-DB 11	A/CB 90%	J-QF-CB 11	C	J-QF-DB 11	A		
AG-P-DB 12	A/CB 90%	J-CB 12	C	J-DB 12	A/CB 90%	J-QF-CB 12	C	J-QF-DB 12	A		

Failure types: A = Adhesive failure (failure at the cylinder-base interface), C = Cohesive failure (failure within the cylinder or base material). CB = Cohesive failure of material within the plaster base. CC = Cohesive failure of the material in the applied cylinder. CB% = Approximate percentage of the surface area of the 50 mm Ø circle of base material having left the base and being present on the pulled off cylinder. CC% = Approximate percentage of the 50 mm Ø circle surface area where cylinder material was observed remaining on the plaster base. X = Indicates either a spoiled specimen or a damaged base from which an accurate assessment could not be made

Figure 10c shows specimens from sample group AG-KF-DB, which featured gel/fibres and primer on a dirty base. Specimens in this group all showed partial cohesive failure with varying extent of base material evident on the cylinders as shown in the top and bottom images; it can be seen in the close-up on the metal block of the top image specimen that the cured product is pliable rather than stiff.

Figure 10d shows specimens from sample group AG-P-DB, with just primer on dirty bases. This group also showed partial cohesive failure on all specimens with base plate material evident on the pulled-off cylinders to varying extents (as shown on both example specimen images). The Sika glue on the metal block is clearly visible in the top specimen image. Figure 10e shows from left to right, the template with aperture on the top of a base, a clean base specimen with just primer, a clean base specimen with gel/fibres/primer and a close-up further illustrating the ductility of the cured gel product, which can be manoeuvred by hand and is not rigid. This ductility allows movement in in-situ applications as building

elements, to which fibrous plaster ceilings are connected to, commonly deflect over time.

3.4 Jesmonite groups with and without quadaxial fibres

Selected images showing the range of failure types from sample groups J-CB, J-QF-CB, J-DB and J-QF-DB are shown in Figure 11. The ‘criss-cross’ keying to aid bonding between the plaster base and cylinder is particularly visible in these images. Figure 11a illustrates specimens from group J-CB, featuring Jesmonite on a clean base. All specimens in this sample group failed in a cohesive manner with varying quantities of bulk material pulled out of the plaster base (as shown in the top and bottom specimens), with one exception which featured largely adhesive failure, with approximately 80% of the circular area being smooth material and 20% of the circular area was partial cohesive failure with a thin layer of material was pulled off the base plate (as shown in the middle specimen image). A strong ‘key’ applied to the base



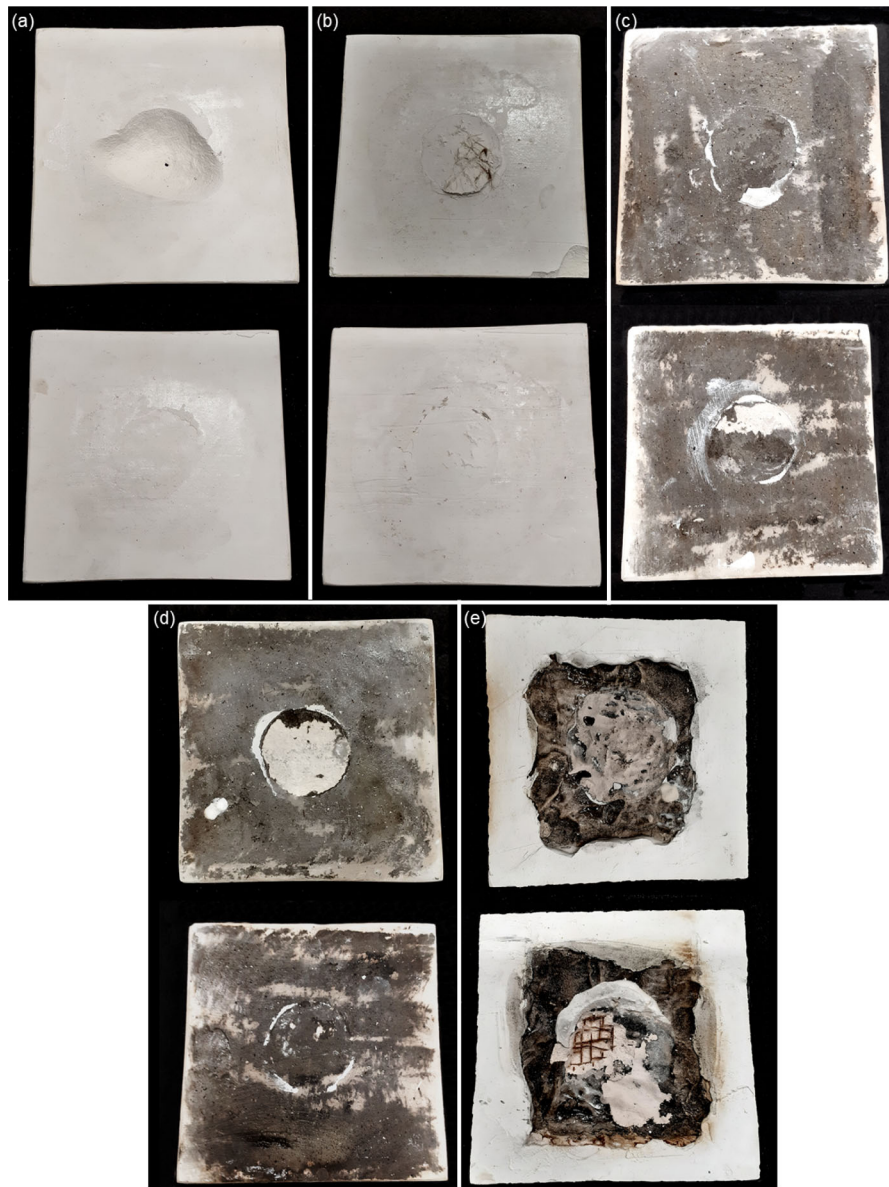


Fig. 8 Tested bases (dimensions 150 mm × 150 mm) from groups BP-CB, BP-HF-CB, BP-DB, BP-HF-DB and BP-HB/BP-HF-HB. **a** Group BP-CB; failure ranged from cohesive in the base material (top) and adhesive (lower). **b** Group BP-HF-CB, partial cohesive failure of the applied cylinder (top) and adhesive failure (lower). **c** Group BP-DB featured adhesive

failure at the cylinder-base interface (top) and partial cohesive failure of base material (lower). **d** Group BP-HF-DB failed in an adhesive manner (bottom) and partial cohesive failure of base material (top). **e** Group BP-HB/BP-HF-HB, adhesive failure (top) and partial cohesive failure of the base exposing hessian fibres (lower)

plate prior to cylinder application is in evidence and while intuitively one might consider this would strengthen the bond between the applied cylinder and clean base plate which is typically the case, it has not with this specimen. This could be explained by a

difference in the material mix in the applied cylinder on this one anomaly which led to a less strong adhesive bond than the other sample group specimens.

Figure 11b depicts specimens from group J-QF-CB, featuring Jesmonite and quadaxial fibres on a clean



Fig. 9 Tested specimens from groups AP-CB, AP-QF-CB, AP-DB, and AP-QF-DB. **a** Group AP-CB, cohesive failure of base material. **b** Group AP-QF-CB, cohesive failure in bases. **c** Group AP-DB, partial cohesive failure of base material (top, middle) and cohesive failure (bottom images). **d** Group AP-QF-DB,

partial cohesive failure of base material (top, middle) and cohesive failure of base material (bottom). **e** Clean based (left) and dirty (right) specimens. Cylinders 50 mm \varnothing and base dimensions 150 mm \times 150 mm



Fig. 10 Tested specimens from groups AG-KF-CB, AG-P-CB, AG-KF-DB, and AG-P-DB. **a** Group AG-KF-CB, adhesive and cohesive failure with partial cohesive failure of base material. **b** Group AG-P-CB, cohesive failure with base material removed (top) and partial cohesive failure of base material (lower). **c** Group AG-KF-DB, partial cohesive failure of base

material. **d** Group AG-P-DB, partial cohesive failure with base material evident on cylinders. **e** Left to right: template with aperture on a base, a clean base specimen with just primer, a clean base specimen with gel/fibres/primer and a close-up illustrating the ductility of cured HPCP RE Aramid GelTM. Cylinders 50 mm Ø, base dimensions 150 mm × 150 mm



◀ **Fig. 11** Tested specimens from groups J-CB, J-QF-CB, J-DB, and J-QF-DB. **a** Group J-CB, cohesive failure in the base (top and lower) with one exception of largely adhesive failure where ‘keying’ is evident (middle). **b** Group J-QF-CB, cohesive failure in base material. **c** Group J-DB, cohesive failure (top) and partial cohesive failure of base (middle, lower). **d** Group J-QF-DB, partial cohesive failure of base material (top, middle), adhesive failure (lower). Cylinders 50 mm Ø, base dimensions 150 mm × 150 mm

plaster base. Specimens in this group exhibited cohesive failure with a range of bulk quantities of material pulled out of the base shown in the upper and lower example specimens depicted; the middle image shows the one example within the group of partial cohesive failure with a small quantity of base plate material in evidence attached to the cylinder and metal block.

Figure 11c illustrates specimens from group J-DB, featuring Jesmonite on a dirty base. Group J-DB specimens largely exhibited partial cohesive failure of the base material with the circular area of base material largely being removed (middle and bottom images). The middle image shows an example of cohesive failure with a bulk quantity of base material being removed, this may again be due to less dirt applied to the central circular area on this specimen.

Figure 11d depicts specimens from group J-QF-DB, with Jesmonite and quadaxial fibres applied to a dirty base. This group featured a mix of adhesive failure and partial cohesive failure of the base material, with a small thin quantity of base material evident in the top and middle example specimen images and adhesive failure shown in the bottom example specimen images. It can be observed that there is a varying level of keying being applied ranging from very evident (middle specimen) to not in evidence (top specimen images and the adhesive failure in the bottom specimen images).

3.5 Failure type visual summary

Figure 12 contains a visual summation of the failure types of all sample groups which were listed in detail for each specimen in Table 4. The colour coding fill within the sample boxes represents the colour coding of the predominant type of failure within the group, with the box containing a gradient colour fill if two failure types featured significantly within a sample

group. Sample group boxes are border-coloured in accordance with the matrix material, with colours matching those used in the bar colour-fills in Figure 5, Figure 6 and Figure 7. Sample group boxes also contain the mean loading in kN for hat group required to pull-off the applied cylinder from the base. A key for matrices, fibres and bases is contained in the yellow boxes. Full cohesive failure within applied cylinder material did not occur throughout the tests.

4 Discussion and application to the fibrous plaster industry

This study investigates the bonding of a repair material administered in situ to an existing historic and aged, perhaps degraded, fibrous plaster element. The loading in particular provides crucial quantification to support the existing commercial practice of repairing and maintaining fibrous plaster ceilings in historic and heritage buildings, which has been based upon experience, observation and empirical understanding of historic and current practice.

It can be observed that there was variation in the results for all sample groups, with groups typically showing a coefficient of variation of around 20% for load and strength and up to approximately 60% for group BP-HF-DB. Variation was higher still when evaluating work done. Results in this study highlight the inherent variation within the materials involved and the presence of variation reflects the variability of real-life commercial practice where materials are mixed on site, quite often in very narrow and confined spaces which are difficult to access and manoeuvrability may only be possible and safe by harness, where it is not practically or realistically possible to weigh constituents consistently.

It should be emphasised again that the aim of this study was not to directly compare the featured methods of repair to each other, but to examine and quantify material properties and potential types of failure. The methods and materials investigated for repairing historic fibrous plaster elements are different and distinct and are all established and effective methods. The methods will therefore be discussed further in individual matrix material sub-sections—Beta Plaster, Alpha Plaster, Re Aramid Gel™ and Jesmonite.- and the sample group test results related to that method. It should be further emphasised that the

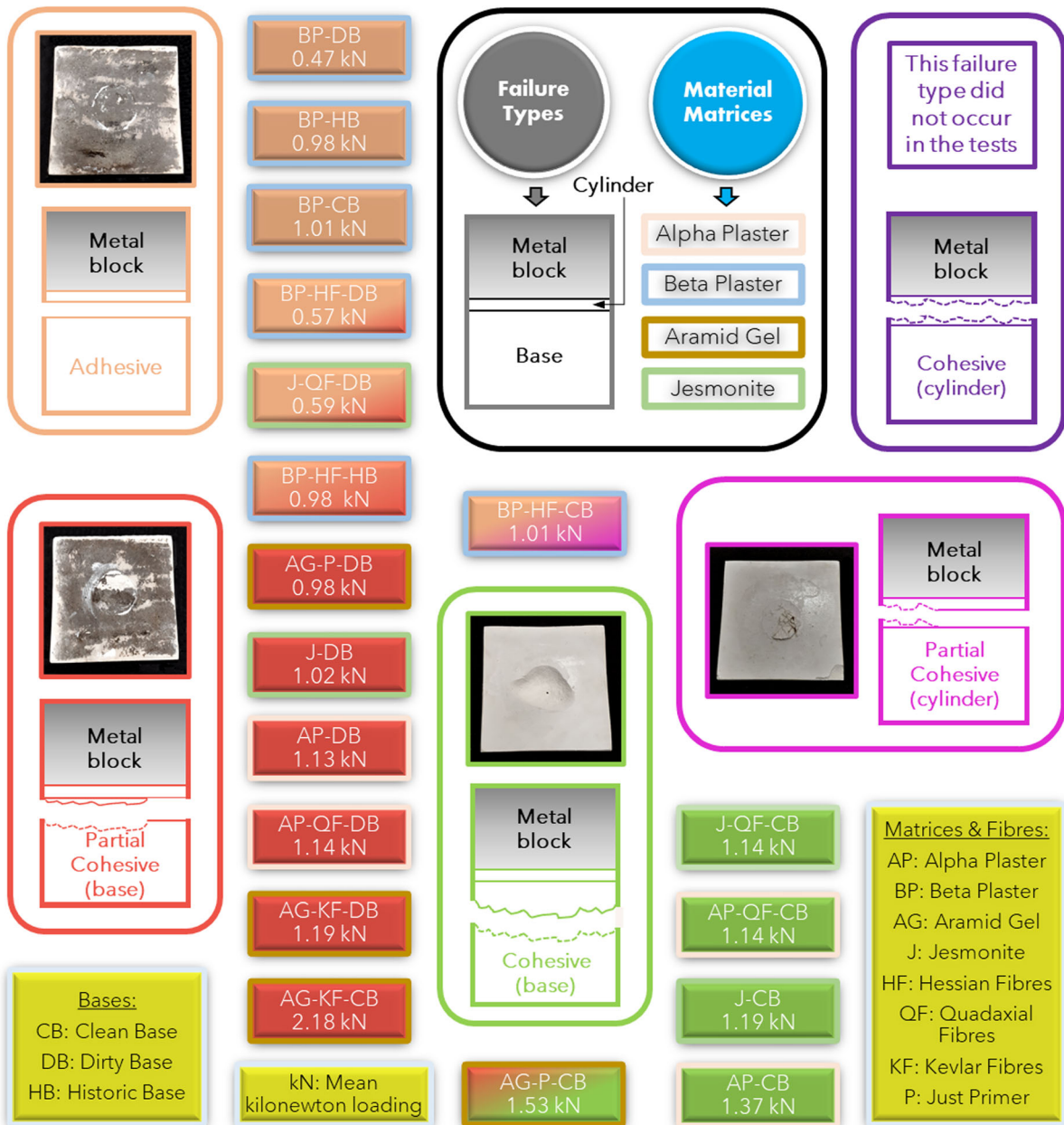


Fig. 12 Visual summary of the predominant failure types for each sample group. Sample group name boxes are fill-coloured to indicate failure type and border-coloured to indicate matrix

material. Sample group boxes also contain the group mean loading required to pull the cylinder off from the base.

discussion sections of this study are based upon results attained in a controlled, consistent laboratory environment and that evaluation of results does not seek to form any sort of partial influence or replacement to full on-site detailed surveillance and inspection by experienced industrial professionals.

All fibrous plaster ceilings, and the buildings in which they are contained, are individual and separate entities which may vary considerably in dimensions, shape and design and contain various features such as domes and inclined planes. Individual building design and fibrous plaster ceiling creation result in notably

different roof spaces and auditorium environments and capacities, which would affect other aspects over long time periods such as temperature and relative humidity conditions. Variability in material performance and in-situ spatial dimensions and environmental conditions inherently make it challenging to specify programmes of works and schedule key stage inspections.

Thermal and hygric variations can affect building environments significantly. Varying temperature and relative humidity conditions in spaces such as theatres will play a role in affecting the topside surface of an in-situ fibrous plaster ceiling, with the environment being affected by varying human occupancy (for example during a performance with maximum capacity attendance levels) and external weather conditions affecting the environment within a roof space, which may not be fully airtight. Daytime temperature variations influenced by solar conditions can be very significant with potentially very high summer temperatures in roof spaces possible; again, this would vary from building to building depending on aspect and elevation design, dimensions and orientation.

Moisture ingress, co-efficient of contraction / expansion and wider conservation considerations such as fungal degradation are also considerations in building spaces. This study focused upon adhesion between existing material and new material interfaces represented by the cylinder/base interface in a laboratory environment. Further conservation considerations are currently under investigation by the authors including the monitoring of temperature and relative humidity conditions within theatre environments both below and above fibrous plaster ceilings (further adhesion tests involving varying relative humidity levels in line with monitoring data are planned) and the reader is referred to [30] for an in-depth investigation of moisture and fungal degradation. Further in-situ parameters currently under consideration by the authors are acoustic impacts causing movement and vibrations of fibrous plaster ceilings and alterations carried out as a result of installing or updating light and sound systems which would vary from one venue to another.

4.1 Beta plaster sample groups with and without hessian fibres

This sample group represented the method of applying new fibrous Beta plaster wads and the bonding of the

new plaster-soaked hessian scrim to the upper side of an in-situ fibrous beta plaster element. This would explain why the only example of partial cohesive failure evident in samples was in the sample group BP-HF-CB, clean base, as the cylinder was the same material as the base. It is also understandable that the failure type in the sample groups is predominantly adhesive—specimens are failing at the cylinder-bond interface because both materials are Beta plaster—no one material is pulling the other causing full cohesive failure, whereas in the other sample groups the cylinder material is stronger and typically pulls an extent of base material out in failure. Sample groups BP-DB and BP-HF-DB (dirty bases) both failed at approximately 0.5 kN—therefore, essentially around 50 kg—with BP-HF-DB being slightly higher having hessian fibres.

While it may be tempting to look at Fig. 5 and Fig. 6 and note that this sample group has values which are not as ‘high’ as some others, one has to consider the differences in application and fibrous plaster material loading scenarios. This pull-off test in this particular sample group is representing a vertical hessian wad being draped over existing in-situ material, a quite different application to placing soaked scrim or spraying a thin, wide-area covering of repair material directly on to an existing ceiling element. The loading provided by a fibrous plaster ceiling element should also be considered; taking a density value of 800 kg/m³ to represent both traditional Beta fibrous plaster and timber laths, a square metre ceiling element of typical 6 mm thickness would weigh in the region of 5 kg. Considering that in historical practice, four wads are applied per square metre, this study has determined that one new wad, under vertical dead loading, is more than adequate to support the square metre of ceiling, at what is potentially the weakest point of the wad—the interface between the applied wad and the existing ceiling. Therefore, assuming that four wads per square metre are affixed in practice, there is a very large safety factor and redundancy in the fibrous plaster structure with vertical dead loading. Hence, the use of traditional Beta plaster hessian wads as a ‘like for like’ repair method is appropriate and effective at the wad-ceiling interface. (Note that although heavy decorative features weigh significantly more than typical ceiling elements, other methods of restraint such as wire restraints and steel washers are used for those exceptional elements).

Naturally, vertical dead loading is not the only load case an in-situ fibrous plaster ceiling would be subjected to. Lateral loading due to potential movement of the building envelope walls over long time periods (possibly due to subsidence) or movement/deflection in supporting structural beam elements, plus additional loading and risk of damage from lighting and sound equipment being installed or potential loading due to water ingress or leaks also have to be considered and would utilise the redundancy. The large redundancy in the wads is also an asset when the additional possibility of material (particularly plant-based fibres) degradation due to moisture or fungal attack over a very long time period is considered, with the wads losing tensile capacity as a consequence. An option for further increased redundancy to counter long-term degradation could be introduced by using spacings of 0.5 m centres for new works.

4.2 Alpha plaster sample groups with and without quadaxial fibres

This group represents Alpha plaster, which has a typical bulk density of $1100 \pm 100 \text{ kg/m}^3$, being applied with quadaxial fibres in a thin layer on a ceiling element. It is interesting to note that this sample group shows the least variation in results between clean base samples and dirty base samples, with the two being comparable to each other in loading/strength and the other groups generally witnessing the detrimental effect of a dirty base. Alpha plaster (the applied cylinders) is stronger than beta plaster, therefore it was not surprising to see these sample groups exhibit entirely cohesive failure in the beta plaster bases on the clean base sample groups (AP-CB, AP-QF-CB) and partial cohesive failure on the sample groups with dirty bases (AP-DB, AP-QF-DB) as the stronger Alpha material pulled out the Beta. However, when on a new base, the difference in tensile load/strength is not large (Fig. 5 and 6).

In an in-situ application to historic material, it is not desirable to use a material which is stiff and lacking in ductility in large quantities. This could lead to problems with regards to movement of the building structure or in the surrounding areas of the historic material itself. Any applied new material is also adding dead loading to the original plaster. An advantage of using alpha plaster in practice is the high strength to weight ratio, requiring little water and

allowing for thinner application of new material and avoiding adding large amounts of dead loading to historic ceilings. Stiff material applied in excessive thicknesses is neither needed in terms of performance under loading, or desired as the excessive introduction of new stiff material may alter existing load paths [33]. It may also induce cracks in surrounding original material when any building movement or movement in the original plaster occurs; typically historic buildings with fibrous plaster ceilings do not contain movement joints. Therefore, the ability of alpha plaster with reinforcing fibres to result in the placement of soaked scrim in very thin laminations of little over a millimetre is favourable and sympathetic to existing historic material.

The new alpha plaster lamination place on the ceiling is designed to improve the flexural strength of the aged ceiling. The difference in flexural strength was demonstrated by [15], with the mean flexural strength of alpha plaster samples (using water) with two layers of hessian fibres being 5.96 MPa as opposed to beta plaster being 3.77 MPa. Variation can also be applied in the manufacture of the repair material, with the option of using an acrylic polymer (such as AC300) as a substitute for water. The application of soaked fibre mats on to the topside of ceilings in-situ naturally assists adhesion as gravity works in favour of the application method. The presence of quadaxial fibres as a modern alternative to plant-based hessian scrim also presents the potential for greater resistance to fungal-induced degradation over a very long time period.

4.3 HPCP RE Aramid GelTM sample groups with DuPontTM Kevlar® fibres and HPCP CO S-20TM acrylic primer

This sample group represents HPCP RE Aramid GelTM containing DuPontTM Kevlar® fibres (typical fibre density 1400 kg/m^3) as an alternative to new plaster being applied to fibrous plaster elements, typically sprayed on a ceiling topside in a thin layer. This sample group experienced the largest pull-off loads and strengths within the study, with pull-off loads exceeding 2 kN on clean bases and 1 kN on dirty bases, denoting a strong interfacial bond between the product and plaster base.

With the applied cylinder material being significantly stronger than the Beta plaster in the bases,



specimens generally exhibited either full cohesive failure (notably in clean base samples) and largely partial cohesive failure with small quantities of the Beta plaster in the base being evident on the pulled off cylinders.

As mentioned, it is not desirable to apply a notably stronger material than historical plaster if that stronger material has high stiffness; it is preferable for applied repair material in a cured state to possess flexibility and ductility. Post testing, it was demonstrated with hand manipulation that the cured gel material on the metal blocks could be manoeuvred with ease. This demonstrable ductility will enable the gel material, whether applied to ceiling panels or encapsulating existing wads, to accommodate building movement in an in-situ application and not restrict the original plaster in any way by introducing rigidity. The gel is an aqueous acrylic emulsion containing Kevlar fibres, and fibres may be randomly distributed in the emulsion, reducing the stiffness of the composite. Fibres have flexibility, ductility, toughness, and yield under loading, properties which are understood particularly from their established use in protective body armour [28, 34]. It is this which makes kevlar suitable for fibrous plaster repair application as opposed to alternatives such as carbon fibre which may be even stronger—but also stiffer [35].

4.4 Jesmonite sample groups with and without quadaxial fibres

This group represents Jesmonite as another alternative to plaster being applied to historic ceiling elements. Jesmonite is denser than Beta plaster and results in this study show that Jesmonite is moderately stronger than Beta plaster in the pull-off tests. Therefore also considering the flexibility of the Jesmonite material and the ability to apply in thin laminations, it is a sympathetic modern replacement alternative and would not be considered too strong or, crucially, stiff to be incompatible with historic gypsum plaster. In clean base sample groups J-CB and J-QF-CB, failure was predominantly cohesive, with the slightly stronger Jesmonite pulling out quantities of Beta plaster from the bases. With dirty base sample group J-DB, the failure was typically partial cohesive, with smaller amounts of base material observed on the Jesmonite cylinders.

Interestingly, dirty base sample group J-QF-DB, which has quadaxial fibres as well as Jesmonite, resulted in several specimens failing in an adhesive manner and an overall mean lower strength/loading capacity than group J-DB (just Jesmonite). This highlights the difference that ‘keying’ can make in the bonding of newly applied material to historic in-situ material, with the specimens failing in an adhesive manner not displaying markedly clear keying effects and having a smooth surface appearance as can be seen in the upper and lower specimen example images in Fig. 11d. Whereas, in contrast, the middle specimen shows marked and distinctive keying. It is suggested that with more marked keying, more specimens in sample group J-QF-DB would have exhibited partial cohesive failure in the base material.

5 Conclusions

This study has examined four highly significant materials used in the repair and conservation of culturally important fibrous plaster ceiling elements in historic and high status buildings. Materials examined were Alpha Plaster (with and without quadaxial fibres), Beta Plaster (with and without hessian fibres), HPCP RE Aramid GelTM with DuPontTM Kevlar[®] fibres (and HPCP CO S-20TM primer) and Jesmonite (with and without quadaxial fibres) being applied to bases simulating original and aged historic material in-situ. Fibre-reinforced plaster can be applied as wadding ties (or ‘wads’) suspended from roof structures and attached to plaster element topsides or applied as thin fibre-reinforced laminations; Jesmonite and HPCP RE Aramid GelTM are typically thinly applied over a topside area of in-situ plaster elements. The results of pull-off tests have provided quantification of repair material adhesive properties and identified modes of failure for the interface between newly applied cured repair material and historic aged material. Dirty, aged in-situ material commonly exhibited adhesive failures with new material, or partially cohesive failures with small amounts of aged base material being pulled off in the tests by stronger material on applied cylinders. Stronger new material applied to cleaner bases led to cohesive failure of base material, with bulk quantities of base material pulled out. Loading required to pull applied material from base material (representing aged in-situ material)



ranged from 0.5 kN for Beta plaster—which demonstrates and confirms the high level of redundancy in the vertical dead-loading of existing examples of historic application of Beta fibrous plaster wads in roof spaces attached to ceiling topsides—to over 2 kN for HPCP RE Aramid Gel with fibres.

A repair material having a higher strength—weight ratio enables thin application. It is also important for applied repair material which is significantly stronger than the aged material to be ductile and yield, as opposed to possessing high stiffness, which the cured Re Aramid Gel™ material satisfied as demonstrated. Ductility in thinly applied stronger material would avoid the potential alteration of existing load paths and potential problems in surrounding areas of aged material. Alpha plaster and Jesmonite proved to be moderately stronger than Beta plaster in the pull-off adhesion tests, and they can be applied in thin laminations, lessening added dead loading.

This study adds to existing fibrous plaster experience and knowledge by providing data and analysis from a robust investigation of nearly 200 specimens tested in a controlled laboratory environment. Each in-situ fibrous plaster ceiling and historic building will have unique environmental conditions and roof spaces; surveillance and inspection should always be carried out for each case. The contribution of scientific data and increased knowledge of potential failure mechanisms will aid fibrous plaster conservation by complementing empirical observation to inform the specification of repair materials and promote the longevity of fibrous plaster ceilings for future generations to safely enjoy.

Acknowledgements The authors gratefully acknowledge support from the Leverhulme Trust through Grant Number RPG-2021-147, Historic England and the Climate-Resilient Energy Secure and healthy built environments (CREST) project. CREST is supported by a Going Global Partnerships—Collaborative Grant from the British Council’s Going Global Partnerships programme [Grant Number 877766384]. The authors would also like to express their gratitude to the following companies for generously contributing time and materials for this research: Hayles and Howe Ornamental Plasterwork and Scagliola Ltd., Bristol, United Kingdom, with additional thanks to Robin Harrison for sharing expertise and arranging visits to theatre venues in the United Kingdom to view surveying and repair work. Locker and Riley Artisans in Plaster, South Woodham Ferrers, Chelmsford, United Kingdom, with additional thanks to Gary Buckley for sharing expertise. Historic Plaster Conservation Services Ltd., Port Hope, Ontario, Canada, with thanks to Rod Stewart, Eric Stewart and Masumi Suzuki for

the image in Figure 1f. Ornate Plaster (London) Ltd., Farnham, Surrey, United Kingdom. The authors additionally thank Richard Ireland, Plaster & Paint: Consultancy & Conservation of Historic Buildings, UK for the use of the image in Figure 1e. Thanks also goes to William Bazeley and Neil Price within the Department of Architecture and Civil Engineering, University of Bath, for providing technical support during this study. The individual pull-off test data supporting this manuscript is available from the dataset for the results of fibrous plaster tests contained in the University of Bath Research Data Archive with the reference <https://doi.org/10.15125/BATH-01275>.

Open Access This article is licensed under a Creative Commons Attribution 4.0 International License, which permits use, sharing, adaptation, distribution and reproduction in any medium or format, as long as you give appropriate credit to the original author(s) and the source, provide a link to the Creative Commons licence, and indicate if changes were made. The images or other third party material in this article are included in the article’s Creative Commons licence, unless indicated otherwise in a credit line to the material. If material is not included in the article’s Creative Commons licence and your intended use is not permitted by statutory regulation or exceeds the permitted use, you will need to obtain permission directly from the copyright holder. To view a copy of this licence, visit <http://creativecommons.org/licenses/by/4.0/>.

References

1. Payne EM (2020) The conservation of plaster casts in the nineteenth century. *Stud Conserv* 65(1):37–58. <https://doi.org/10.1080/00393630.2019.1610845>
2. Millar W (1897) *Plastering plain & decorative*, 1998 Repri. Dorset, Donhead
3. Stewart J, et al. (2019) *Historic fibrous plaster in the UK. Guidance on its care and management*. Hist. Engl. <https://historicengland.org.uk/images-books/publications/historic-fibrous-plaster/heag269-historic-fibrous-plaster/>.
4. Brookes S (2021) Historic plaster ceilings. Part 1: development and causes of failure. *Struct Eng* 99(3):20–24
5. BBC (2023) Apollo theatre - ceiling collapses during show in London. BBC, 2013. <https://www.bbc.co.uk/news/uk-england-25458009>. Accessed Jun 12, 2022
6. Urquhart C, Williams R (2023) Apollo theatre collapse injures more than 80 people in London’s West End. *The Guardian*, 2013. <https://www.theguardian.com/uk-news/2013/dec/19/apollo-theatre-london-balcony> Accessed May 15, 2023
7. France A (2019) Savoy ballroom ceiling collapses, showering black-tie auction guests with debris. *Evening Standard*, <https://www.standard.co.uk/news/london/savoy-ballroom-ceiling-collapses-showering-blacktie-auction-guests-with-debris-a4082701.html>. Accessed Jun. 12, 2022.



8. ABTT (2015) ABTT guidance note 20 May 2015 advice to theatre owners and managers regarding suspended fibrous plaster ceilings; survey, certification, record keeping etc.
9. Maundrill Z (2021) The effects of different environmental conditions on hessian in historic fibrous plaster wads. University of Bath
10. Brookes S, Clark K, Frostick R, Ireland R, Randall L (2020) The plaster ceilings of buckingham palace and windsor castle: their construction, condition and conservation. In: 12th international conference on structural analysis of historical constructions. <https://doi.org/10.23967/sahc.2021.293>.
11. Bowley B (1994) Historic ceilings. *Struct Surv* 12(2):24–28. <https://doi.org/10.1108/02630809410049112>
12. Ireland R (2020) Investigation and assessment of decorative plaster ceilings. *J Build Surv Apprais Valuat* 9(3):228–245
13. Huq T et al (2010) Fabrication and characterization of jute fiber-reinforced PET composite: effect of LLDPE incorporation. *Polym - Plast Technol Eng* 49(4):407–413. <https://doi.org/10.1080/03602550903532174>
14. Masrani SK, McKiernan P, McKinlay A (2020) Strategic responses to low-cost competition: technological lock-in in the Dundee jute industry. *Bus Hist* 62(6):960–981. <https://doi.org/10.1080/00076791.2018.1502750>
15. Ngah SA, Dams B, Ansell MP, Stewart J, Hempstead R, Ball RJ (2020) Structural performance of fibrous plaster. Part 1: Physical and mechanical properties of hessian and glass fibre reinforced gypsum composites. *Constr Build Mater* 120396
16. Jesmonite (2022) Jesmonite AC100. Jesmonite Limited, Shropshire, 2022. <https://jesmonite.com/how-sustainable-friendly-is-jesmonite-your-faqs-answered/> Accessed Oct 26, 2022
17. HCPS (2022) Reinforcement: HPCS RE aramid Ge1™ for reinforcing and stabilizing fibrous plaster. Historic Plaster Conserv Serv. <https://www.historicplaster.com/products/reinforcement/> Accessed Oct. 27, 2022
18. Stewart R (2022) HPCS RE aramid Ge1™ for reinforcing and stabilizing fibrous plaster. Historic Plaster Conservation Services, <https://www.historicplaster.com/products/reinforcement/>
19. Bungey JH, Madandoust R (1992) Factors influencing pull-off tests on concrete. *Mag Concr Res* 44(158):21–30. <https://doi.org/10.1680/mac.1992.44.158.21>
20. BS British Standard (1992) BS 1881–207–1992 Testing concrete - Part 207: Recommendations for the assessment of concrete strength by near-to-surface tests.
21. Industrial Plasters (2023) Prestia classic plaster 2023. <https://industrialplasters.com/collections/prestia-casting-plasters/products/prestia-classic-plaster> Accessed May 09, 2023
22. Saint Gobain Formula (2023) Crystacal R. 2023. <https://www.saintgobainformula.com/product/crystacal-r>
23. Industrial Plasters (2023) Crystacal R plaster 2023. https://industrialplasters.com/products/crystacal-r-plaster?_pos=1&_sid=aa6f31eff&_ss=r (accessed May 09, 2023).
24. Jesmonite (2022) AC100 technical data sheet. MBFG, 2022. https://mbfgfiles.co.uk/datasheets/ac100_tech.pdf Accessed Dec 02 2022
25. Jesmonite Ltd (2023) Jesmonite AC100 technical data sheet. Shropshire, UK, https://www.mbf.co.uk/QL2200.html?gclid=CjwKCAjw3ueiBhBmEiwA4BhspER4_AqqjNSE4HvkXsutY0wLZ9Te9dY9ikmu74XxCmjP_n0MYZKw4BoCaBUQAvD_BwE.
26. Yeung KKH, Rao KP (2012) Mechanical properties of Kevlar-49 fibre reinforced thermoplastic composites. *Polym Polym Compos* 20(5):411–424. <https://doi.org/10.1177/096739111202000501>
27. MatWeb Material Property Data (2023) “DuPont™ Kevlar® 49 Aramid Fiber. MatWeb, <https://www.matweb.com/search/datasheet.aspx?MatGUID=77b5205f0dcc43bb8cbe6fee7d36cbb5&ckck=1> Accessed May 09, 2023
28. Sun G, Chen D, Zhu G, Li Q (2021) Lightweight hybrid materials and structures for energy absorption: A state-of-the-art review and outlook. *Thin-Walled Struct.* <https://doi.org/10.1016/j.tws.2021.108760>
29. Jesmonite Ltd. (2023) Alkali resistant Quadaxial glass. Shropshire, UK. <https://www.notcutt.co.uk/wp-content/uploads/2014/06/AR-Quadaxial-Technical-Data-Sheet-2014.pdf>.
30. Maundrill ZC et al (2022) Moisture and fungal degradation in fibrous plaster. *Constr Build Mater* 369:130604. <https://doi.org/10.1016/j.conbuildmat.2023.130604>
31. Munikenche Gowda T, Naidu ACB, Chhaya R (1999) Some mechanical properties of untreated jute fabric-reinforced polyester composites. *Compos Part A Appl Sci Manuf* 30(3):277–284. [https://doi.org/10.1016/S1359-835X\(98\)00157-2](https://doi.org/10.1016/S1359-835X(98)00157-2)
32. Mushfequr Rahman M, Sharmin N, Khan RA, Dey K, Haque ME (2012) Studies on the mechanical and degradation properties of jute fabric-reinforced natural rubber composite: Effect of gamma radiation. *J Thermoplast Compos Mater* 25(2):249–264. <https://doi.org/10.1177/0892705711405559>
33. Brookes S (2021) Historic plaster ceilings. Part 2: survey, assessment and methods of conservation. *Struct Eng* 99(4):30–33
34. Wang K, Zhu W, Li S, Peng Y, Ahzi S (2022) Investigations of quasi-static indentation properties of 3D printed polyamide/continuous Kevlar/continuous carbon fiber composites. *J Appl Polym Sci.* <https://doi.org/10.1002/app.52758>
35. Yang G, Guo H, Xiao H, Jiang H, Liu R (2021) Out-of-plane stiffness analysis of kevlar/carbon fiber hybrid composite skins for a shear variable-sweep wing. *Appl Compos Mater* 28(5):1653–1673. <https://doi.org/10.1007/s10443-021-09926-7>

Publisher's Note Springer Nature remains neutral with regard to jurisdictional claims in published maps and institutional affiliations.

